



Review

Recent Advances in Flexible Self-Powered Sensors in Piezoelectric, Triboelectric, and Pyroelectric Fields

Yukai Zhou ¹, Jia-Han Zhang ¹ , Feiyu Wang ¹, Jiangbo Hua ¹, Wen Cheng ^{2,*}, Yi Shi ^{1,*} and Lijia Pan ^{1,*}

¹ Collaborative Innovation Center of Advanced Microstructures, School of Electronic Science and Engineering, Nanjing University, Nanjing 210093, China; zhoyukai@smail.nju.edu.cn (Y.Z.); jhzhzhang@smail.nju.edu.cn (J.-H.Z.); fywang@smail.nju.edu.cn (F.W.); jbohua@smail.nju.edu.cn (J.H.)

² School of Integrated Circuits, Nanjing University-Suzhou Campus, Suzhou 215163, China

* Correspondence: wencheng.ee@foxmail.com (W.C.); yshi@mail.nju.edu.cn (Y.S.); ljpan@mail.nju.edu.cn (L.P.)

Abstract: The rise of the Internet of things has catalyzed extensive research in the realm of flexible wearable sensors. In comparison with conventional sensor power supply methods that are reliant on external sources, self-powered sensors offer notable advantages in wearable comfort, device structure, and functional expansion. The energy-harvesting modes dominated by piezoelectric nanogenerators (PENGs), triboelectric nanogenerators (TENGs), and pyroelectric nanogenerators (PyENGs) create more possibilities for flexible self-powered sensors. This paper meticulously examines the progress in flexible self-powered devices harnessing TENG, PENG, and PyENG technologies and highlights the evolution of these sensors concerning the material selection, pioneering manufacturing techniques, and device architecture. It also focuses on the research progress of sensors with composite power generation modes. By amalgamating pivotal discoveries and emerging trends, this review not only furnishes a comprehensive portrayal of the present landscape but also accentuates avenues for future research and the application of flexible self-powered sensor technology.

Keywords: flexible self-powered sensors; piezoelectric; triboelectric; pyroelectric



Citation: Zhou, Y.; Zhang, J.-H.; Wang, F.; Hua, J.; Cheng, W.; Shi, Y.; Pan, L. Recent Advances in Flexible Self-Powered Sensors in Piezoelectric, Triboelectric, and Pyroelectric Fields. *Nanoenergy Adv.* **2024**, *4*, 235–257. <https://doi.org/10.3390/nanoenergyadv4030015>

Academic Editors: Christos Tsamis, Ya Yang and Zhong Lin Wang

Received: 3 June 2024

Revised: 19 August 2024

Accepted: 19 August 2024

Published: 26 August 2024



Copyright: © 2024 by the authors. Licensee MDPI, Basel, Switzerland. This article is an open access article distributed under the terms and conditions of the Creative Commons Attribution (CC BY) license (<https://creativecommons.org/licenses/by/4.0/>).

1. Introduction

Flexible sensors represent a transformative advancement in the realm of sensor technology by offering unparalleled versatility and adaptability across many applications. Unlike traditional rigid sensors, these innovative devices can conform to various shapes and surfaces, which enables seamless integration into curved or irregularly shaped objects, wearable devices, and even implanted into the human body [1–4]. This flexibility opens up a myriad of possibilities from healthcare monitoring to environmental sensing and beyond. Flexible sensors come in various forms that include strain sensors, pressure sensors, temperature sensors, and biosensors, with each tailored to specific applications and requirements. They utilize a diverse range of sensing mechanisms, such as piezoresistance, capacitance, or optics, to detect and measure changes in physical, chemical, or biological stimuli [3,5,6]. In essence, flexible sensors represent a paradigm shift in sensor design by offering outstanding flexibility, functionality, and integration possibilities that hold immense promise for revolutionizing diverse domains ranging from healthcare and robotics to consumer electronics and beyond.

The inconvenience of relying on an external power supply is increasingly impacting the user experience in the development of flexible electronic devices, particularly for wearable and implantable electronic devices, where it may even pose a risk of injury to the user. Self-powered technology that utilizes the polarization property of materials offers greater potential in device structure and sensing mechanisms compared with wireless power technology and solar technology [7–9]. This is due to its ability to derive power from the material itself, which eliminates the need for additional modules and results in a simpler

structure with more stable performance. Additionally, the power generation process of self-powered technology can be leveraged to design new sensing mechanisms [10]. Currently, the extensively researched and utilized self-powered technology is primarily based on piezoelectric, triboelectric, and pyroelectric principles. In general, these power generation methods involve external stimulation, such as temperature changes, mechanical forces, and deformation, to cause the internal polarity of the material to change. This voltage can also serve as a sensing signal for flexible sensors, such as pressure, strain, and temperature. Figure 1 summarizes the number proportions of different power supply modes (excluding hybrid modes) on the Web of Science with the keyword “self-powered flexible pressure sensor” in the past 5 years. It was found that they were mainly based on piezoelectricity, triboelectricity, and pyroelectricity, while other types included thermoelectric and solar cells.

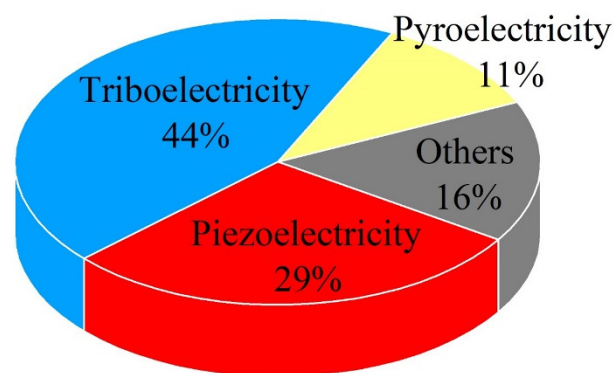


Figure 1. The number proportions of different generation modes used in the last five years.

In terms of the material itself, Figure 2 illustrates the relationships between piezoelectric, triboelectric, and pyroelectric materials, alongside some typical materials and applications. The polarization of piezoelectric and pyroelectric materials is induced by pressure and temperature stimulation. It should be noted that while the crystal structure of piezoelectric materials lacks a symmetry center [7], pyroelectric materials additionally require their own polarization [11]. Additionally, triboelectric materials can generate charge separation through friction between materials with different triboelectric polarity [9] or even within the same material with varying shapes [12]. These distinct material conditions offer unique advantages in device structure, performance, and preparation methods. In order to fully harness the benefits and drawbacks of various power generation methods, an increasing number of researchers showed a preference for self-powered flexible multimode sensors with hybrid generation modes [13–15].

This review endeavored to offer a comprehensive exploration of recent breakthroughs in flexible sensor research across three key self-powered fields: piezoelectric, triboelectric, and pyroelectric, including their respective electric-generation principles, material selection, methodological advancements, performance enhancements, and diversified applications. At the same time, attention is paid to the research progress of flexible sensors with composite self-electric modes, which is rarely mentioned but has an important impact on future research. Moreover, it assesses the enduring obstacles and delineates the potential pathways for future advancements. By undertaking this thorough analysis, this review aimed to shed light on the trajectory of self-powered flexible sensor research and provide valuable insights to guide future endeavors in this vibrant field.

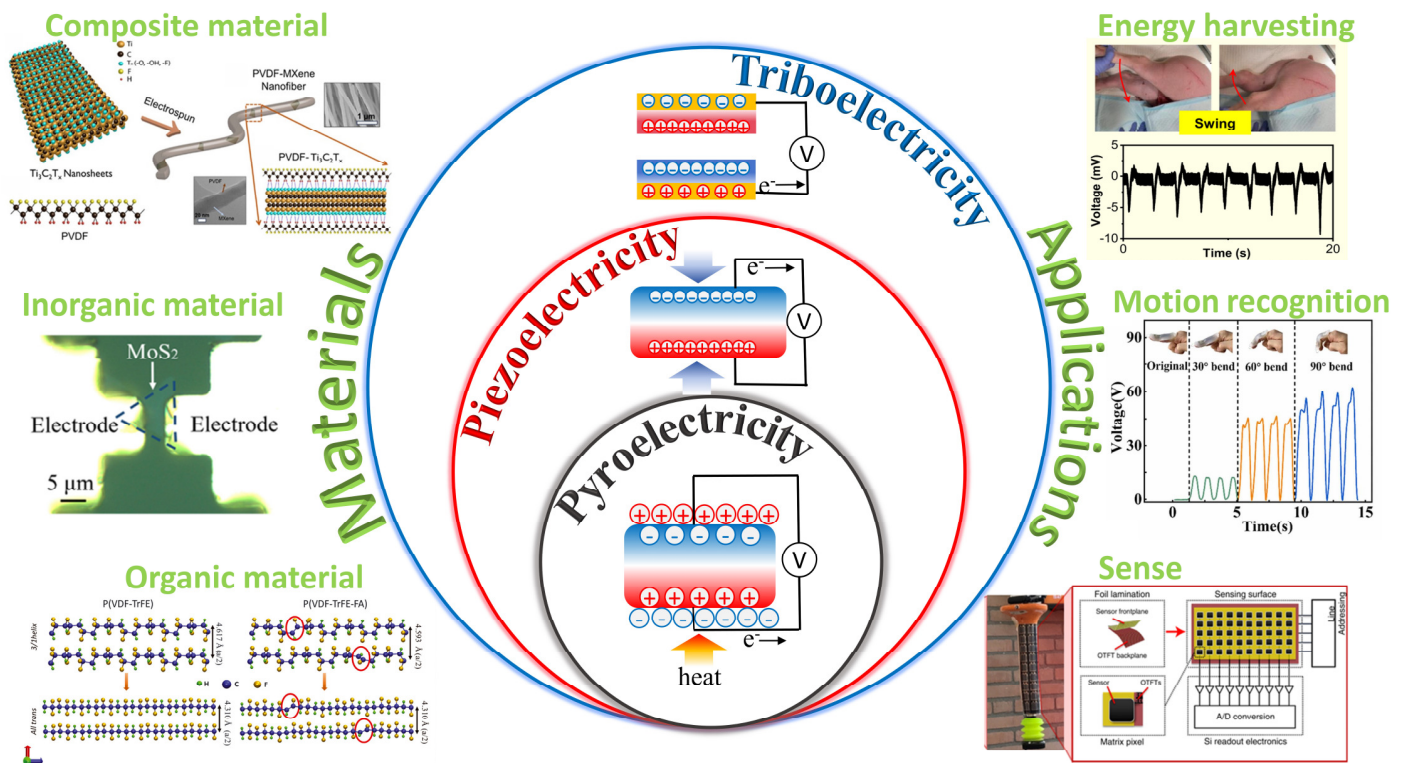


Figure 2. The development of sensors based on three self-powered modes in recent years [16–21]. Reprinted with permission from Ref. [18]. Copyright 2019, Royal Society of Chemistry. Reprinted with permission from Ref. [19]. Copyright 2024, Elsevier. Reprinted with permission from Ref. [20]. Copyright 2024, American Chemical Society.

2. Flexible Piezoelectric Sensor

2.1. Flexible Piezoelectric Technology

As early as 1880, the Curie brothers first discovered the piezoelectric effect while studying quartz crystals. This phenomenon manifests in certain dielectric materials lacking symmetrical center structures, whereby the application of mechanical action or alternating electric fields induces a binding charge or deformation along specific directions. Depending on the generation or reception of charge, the piezoelectric effect is categorized into a positive piezoelectric effect and an inverse piezoelectric effect, which is commonly referred to as the electrostriction effect [22,23]. For the scope of this review, we focus exclusively on the positive piezoelectric effects.

Piezoelectric technology, which is renowned for its compact size, high stability, broad response range, and mechanical robustness, has been at the forefront of power generation methods since its inception [24]. Over decades of development, significant strides have been made in material selection and application fields. As the demand surges for sensors and energy converters characterized by flexibility, lightweight, and adaptability, researchers have embarked on integrating piezoelectric principles with flexible technologies, propelling the concept of flexible piezoelectric nanogenerators (PENGs) [25,26]. Under external strain stimulation, a PENG produces alternating current output through the “33” mode, “31” mode, and so on based on the spatial relationship between the polarization direction and strain direction [27,28].

The essence of flexible piezoelectric technology lies in the exploration of piezoelectric devices capable of maintaining stable performance even under bending and deformation conditions [29]. This puts forward higher requirements for the preparation of piezoelectric materials and the structure of piezoelectric devices. On the one hand, the material needs to have good flexibility and stretching to ensure the stability of the high-quality output charge under a bending or stretching state; on the other hand, the device structure must guarantee

overall structural reliability under external force stimuli [22,24]. In the following, the research progress of flexible organic piezoelectric materials, flexible inorganic piezoelectric materials, and composite materials in the material preparation and device structure are summarized from the perspective of materials.

2.2. Research Progress in Different Materials

2.2.1. Organic Piezoelectric Materials

Organic piezoelectric materials, which are commonly referred to as piezoelectric polymers, encompass a range of amorphous and semi-crystalline polymers. Among these, semi-crystalline piezoelectric polymers stand out for their ability to generate piezoelectricity through the formation of crystalline phases endowed with polarity [30]. Notably, polyvinylidene fluoride (PVDF) and its copolymers, such as P(VDF-TrFE) and P(VDF-HFP), represent prominent examples within this category. Renowned for their lightweight nature and excellent flexibility, they have found widespread application in the realm of flexible piezoelectric sensors. However, their advancement is impeded by inherent challenges, particularly the modest electromechanical coupling performance and demanding polarization requirements [31,32]. Researchers are trying to make a breakthrough by doping or improving the fabrication process. Chen et al. introduced a small amount of fluorinated alkyne (FA) monomer units (<2 mol%) through the dehydrochlorination of chlorofluoroethylene (CFE) in the ternary copolymer P(VDF-TrFE-CFE), which greatly enhanced the electromechanical coupling performance of this kind of material [16]. The FA monomer reduces the conformational transition barrier of the molecular chain. Moreover, due to the small size of FA, it can effectively enter the crystal and inhibit the formation of the long-range ordered ferroelectric phase, thus further improving the electromechanical coupling efficiency of the material (Figure 3a). Under a DC bias field of 40 MV/m, the k_{33} of the P(VDF-TrFE-CFE-FA) tetramer is as high as 88%, and the d_{33} is >1000 pm/V, which is comparable with the electromechanical coupling efficiency of inorganic pressure point ceramics. Yuan et al. treated PVDF with a mechanical directional stress field (MDSF) and made it exhibit a large poling-free piezoelectricity effect and strong electromechanical coupling [33]. They introduced low-concentration PZT ceramic particles into a PVDF matrix, and then prepared nanocomposites through high-speed ball milling and 3D printing processes (Figure 3b). On the one hand, the PZT ceramic particles induced β -phase conversion by mechanical drag activation; on the other hand, the friction and electrostatic effects cause the spontaneous polarization process during ball milling. In addition, mechanical stretching during the 3D printing process further redirects the nanofibers. The d_{33} of the MDSF-treated PVDF nanocomposite membrane sample is about 22 pm/V, which is similar to that of a PVDF membrane with normal high-voltage polarization.

As a burgeoning addition to the realm of organic piezoelectric materials, piezoelectric biomaterials endowed with a polar structure emerge as frontrunners in the development of implantable piezoelectric devices. Their unparalleled combination of superb biocompatibility, biodegradability, and robust mechanical properties positions them as prime candidates for a myriad of biomedical applications [30,34]. This diverse class of materials encompasses a wide array of compounds, including cellulose, chitin, amino acids, peptides, chitosan, proteins, and viruses [35,36]. Li et al. designed piezoelectric bicrystal films based on DL-alanine that was structured into truss-like microstructures through self-assembly under controlled molecular-solvent interactions and interfacial tension [17]. These films can withstand up to 40% tensile strain in various directions by opening and closing the truss mesh, all while maintaining their structural integrity and piezoelectric properties (Figure 3c). This development enabled the creation of stretchable piezoelectric sensors compatible with biological tissues, which were successfully implanted into pig legs for energy harvesting and motion detection.

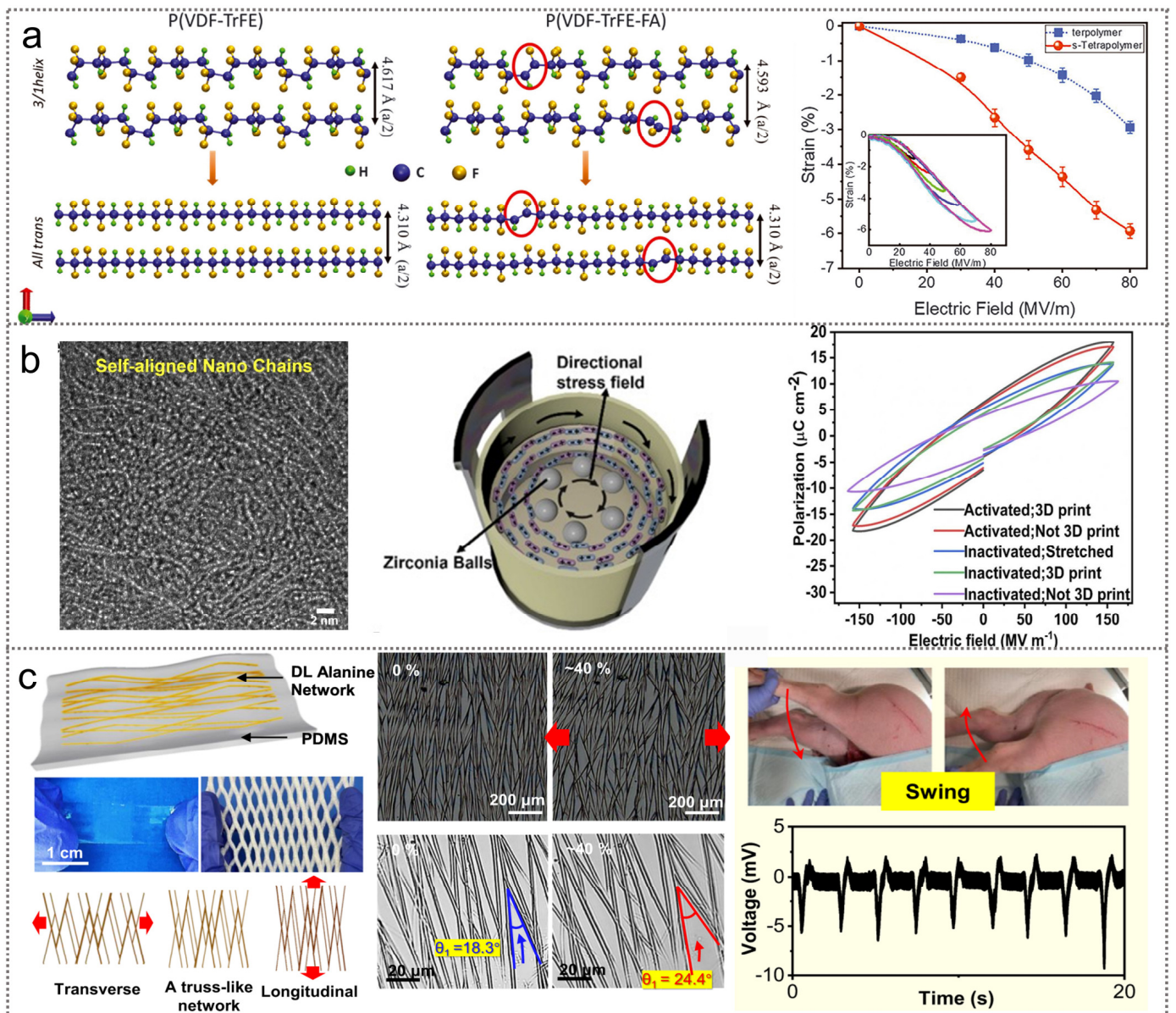


Figure 3. Organic piezoelectric materials in flexible PENG. (a) FA-doped modified terpolymer P(VDF-TrFE-CFE) enhances the piezoelectric output [16]. (b) PZT ceramic particles are introduced into PVDF matrix and generate poling-free piezoelectric effect through MDSF. Reprinted with permission from Ref. [33]. Copyright 2022, Elsevier. (c) The stretchable DL-alanine fiber is self-assembled into a continuous truss-like structure for implantable PENG [17].

2.2.2. Inorganic Piezoelectric Material

Inorganic piezoelectric materials were the earliest-studied piezoelectric materials and have been the most deeply studied. They include long range ordered piezoelectric crystals represented by quartz crystals, ZnO, two-dimensional materials, and polycrystalline piezoelectric ceramics represented by perovskite ceramics (PZT, KNN, NBT) [37]. Compared with organic piezoelectric materials, inorganic piezoelectric materials have higher electromechanical coupling properties, higher mechanical strength, and better stability [22,24]. However, the disadvantages of a high preparation temperature, low flexibility, high brittleness, and toxicity also seriously limit the application of pure inorganic piezoelectric materials in flexible piezoelectric sensors.

To address these limitations and develop high-quality flexible inorganic piezoelectric materials for sensor applications, researchers have explored various fabrication processes from a device-oriented perspective. Liu et al. fabricated a flexible PENG comprising all-ceramic lead zirconate titanate (PZT) deposited on a high-temperature-resistant flexible zirconia ceramic substrate using the sol-gel method [38]. The favorable lattice matching resulted in a smooth surface and a densely packed crystal structure of the PZT ceramic film, which achieved an impressive open-circuit voltage of 105 V. Recently, inspired by the hinge of the bivalve *Cristaria plicata*, Xu used a bionic soft-hard hybrid strategy to build a self-powered sensor with both flexible and high-voltage properties [39]. First, a damage-resistant droplet piezoelectric ceramic was formed by freeze casting on a hydrophobic surface. After polarization, it was placed on a soft circuit that comprised liquid metal to form a stable electrode connection. Finally, an organic silicon polymer (PMDS + Ecoflox) with good wettability and stretchability was used as a soft packaging material to penetrate into the porous ceramic void to produce a strong mechanical interlock (Figure 4a). The resultant sensor epitomized the structural stability by exhibiting remarkable resilience to mechanical stressors, where it withstood 10,000 compression cycles, 5000 stretches, and 5000 twists while maintaining a temperature output. For different stages of device preparation, other novel preparation processes include laser stripping [40], electrospinning [41], mechanical thinning [42], and various stretchable structures [43,44].

It is noteworthy that two-dimensional materials, which emerged as prominent players in the realm of functional materials, offer exceptional advantages in piezoelectricity. First, they boast remarkable mechanical properties, such as enduring strains of more than 10% while maintaining flexibility owing to their thinness [45]. Moreover, as many bulk materials are reduced to two dimensions, especially for odd layers, their structural symmetry is disrupted, which leads to the manifestation of piezoelectric properties [46]. Zhang et al. developed a self-powered sensor for NH_3 detection at room temperature by utilizing an Au-modified MoSe_2 layer and a flexible MoS_2 wafer [47]. Through the piezoelectric properties of single-layer MoS_2 grown via the CVD method on a PET substrate, the sensor generated a maximum output of 62.72 pW under bending strain (Figure 4b). This energy output facilitated NH_3 detection through a high-sensitivity Au- MoSe_2 composite film with fast response times. However, selecting suitable two-dimensional piezoelectric materials warrants attention to factors such as the material band gap, layer count, and lattice orientation [48].

2.2.3. Composite Piezoelectric Material

This discussion highlights a clear distinction between organic and inorganic piezoelectric materials: while the former offer flexibility but lack strong piezoelectric properties and require stringent polarization conditions, the latter exhibit excellent electromechanical coupling yet suffer from rigidity and fragility. This inherent complementarity has spurred efforts toward developing composite materials that seamlessly combine flexibility and electro-mechanical functionality [3,22,30].

One approach involves dispersing inorganic piezoelectric materials, such as particles, nanowires, and nanosheets, within an organic piezoelectric matrix or polymer substrate. These inorganic fillers serve dual roles: enhancing the crystallinity of organic materials as nucleating particles and acting as stress concentration points, thereby facilitating significant local deformation and augmenting the piezoelectric output [49,50]. Jeong et al. incorporated doped BaTiO_3 nanowires into a P(VDF-TrFE) solution, which was then applied onto an ITO/PET substrate using the spinning coating method to fabricate a flexible piezoelectric nanoenergy collector capable of producing an output voltage and current of 14.0 V and 4.0 A (Figure 5a) [51]. Gao et al. employed a dielectrophoretic alignment field on PDMS substrates to prepare BCZT/PDMS composites with lead-free BCZT particles as fillers, which resulted in a high open-circuit voltage of 28.8 V (peak to peak) that was nearly double that of randomly dispersed composites (Figure 5b) [18].

Concurrently, the emergence of organic–inorganic hybrid perovskite structures (OIHPs) presents an intriguing avenue for piezoelectric device development. OIHPs, which are typified by their general formula ABX_3 , where A represents an organic cation, B denotes a bivalent metal cation, and X signifies a halide anion, showcase remarkable potential owing to their high piezoelectricity, lightweight nature, and solution processability [52,53]. Jella et al. conducted a comprehensive investigation into the impact of topographical, electrical, dielectric, and piezoelectric properties on $MAPbI_3$ hybrid perovskite films, with modifications using different halides (Cl or Br) [54]. Their findings demonstrated that halide modification significantly enhanced the piezoelectric properties of OIHP films. In addition, when the content of Cl was increased, the $MAPbCl_3$ phase and $MAPbI_3$ coexisted, while $4Cl-MAPbI_3$ had the highest piezoelectric output performance, with an output voltage of ~ 5.9 V and a current density of $\sim 0.61 \mu A/cm^2$ (Figure 5c).

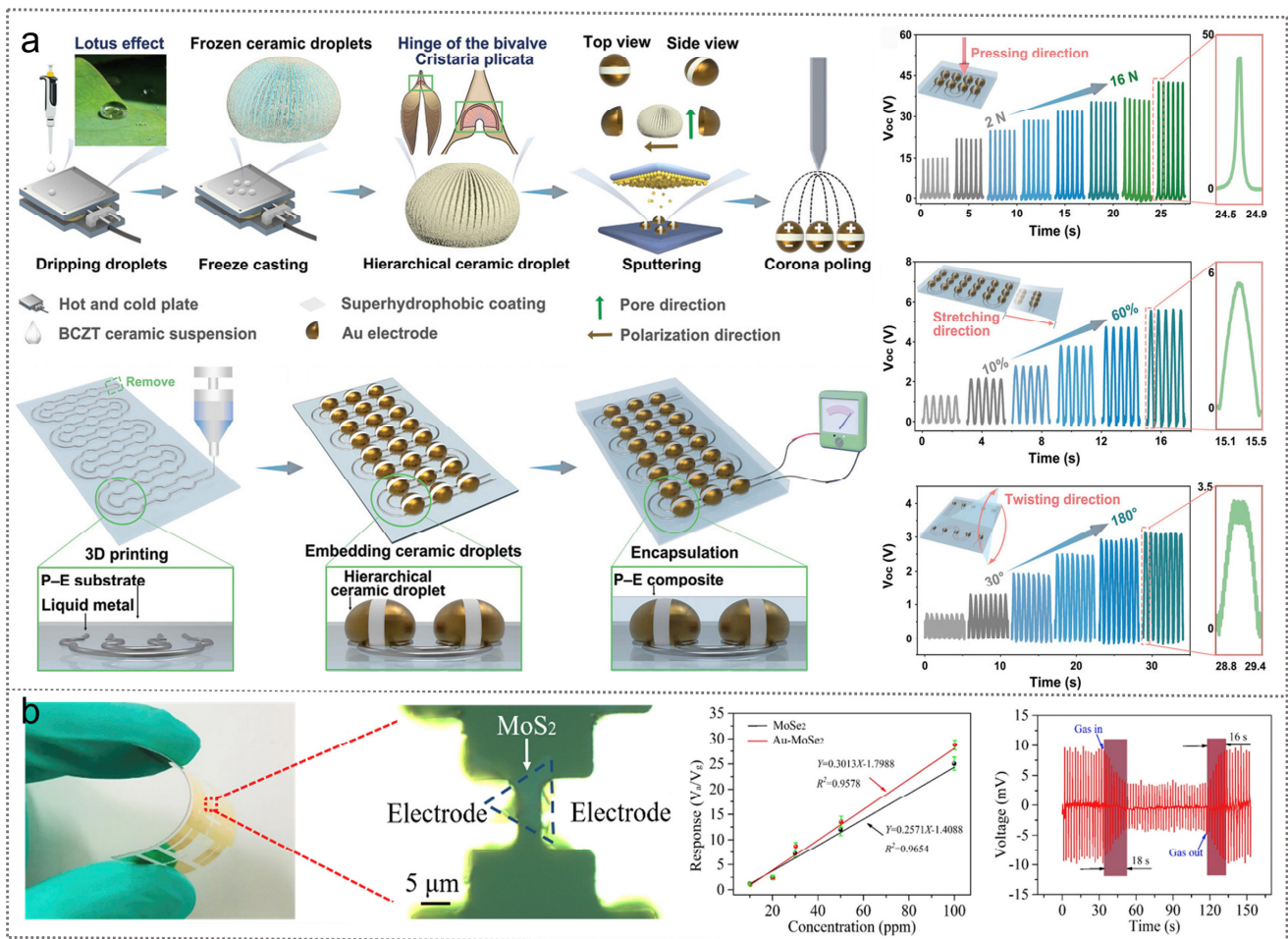


Figure 4. Inorganic piezoelectric materials in a flexible PENG. (a) A kind of self-powered sensor with both flexible and high-voltage characteristics was constructed by using a bionic soft and hard hybrid strategy [39]. (b) MoS₂-based PENG integrated with NH₃ sensor. Reprinted with permission from Ref. [47]. Copyright 2019, Elsevier.

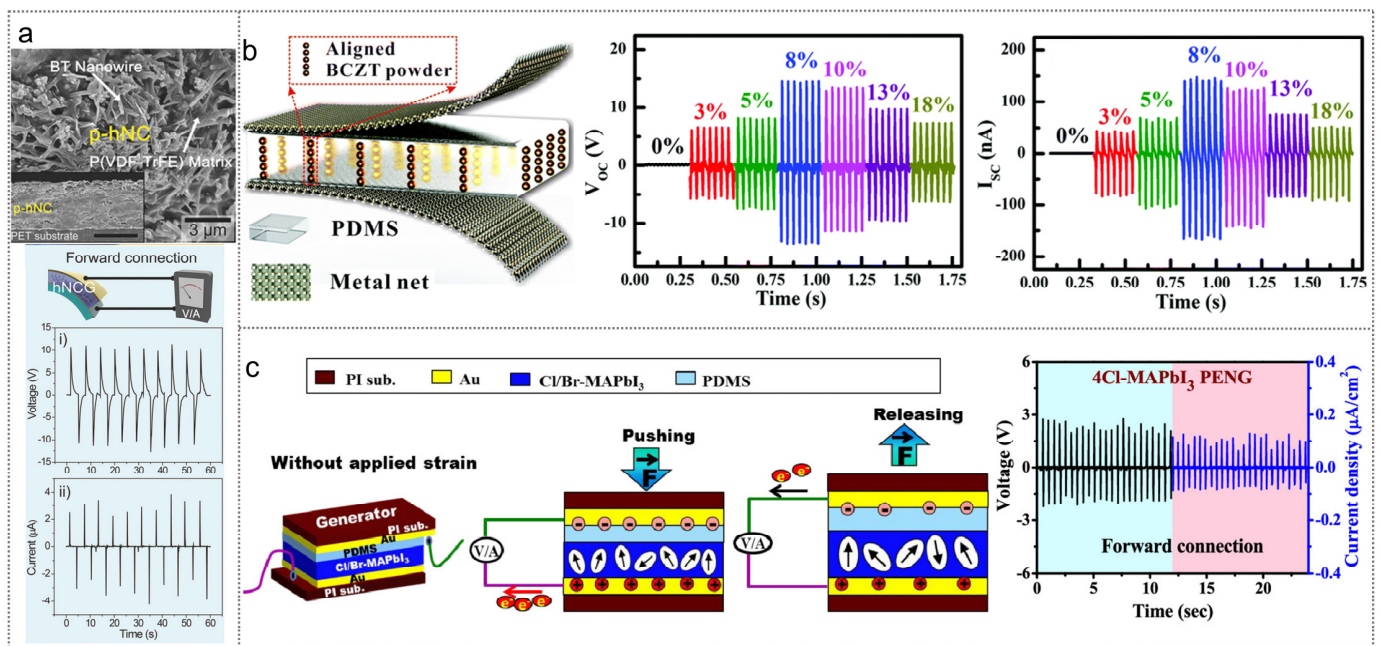


Figure 5. Composite piezoelectric materials in a flexible PENG. (a) BaTiO₃ nanowires were incorporated into P (VDF-TrFE) solution to prepare composite piezoelectric materials. (i) and (ii) represent the test results of the open circuit voltage and short circuit current, respectively. Reprinted with permission from Ref. [51]. Copyright 2018, Wiley–VCH GmbH. (b) BCZT/PDMS composites were prepared by dielectrophoretic alignment field. Reprinted with permission from Ref. [18]. Copyright 2019, Royal Society of Chemistry. (c) Piezoelectric properties of MAPbI₃ hybrid perovskite films doped with different halides (Cl or Br). Reprinted with permission from Ref. [54]. Copyright 2020, American Chemical Society.

3. Flexible Triboelectric Sensor

Triboelectricity, despite its antiquity compared with piezoelectricity, has historically remained underutilized due to its detrimental effects on both industrial processes and everyday activities [55]. However, the pivotal breakthrough by Wang et al., which utilized Kelvin probe microscopy to scrutinize the physical mechanisms behind frictional potential generation, catalyzed a paradigm shift. Their pioneering work led to the development of triboelectric nanogenerators (TENGs), thereby facilitating a more direct and efficient exploitation of this ubiquitous energy source. Their investigation unveiled electron transfer as the primary mechanism underlying friction-induced electricity generation across diverse material states—solids, liquids, and gases. When the interatomic distance between two materials is forced by external contact to be less than the normal bond length, the reduction in the interatomic barrier causes a strong electron cloud between the two atoms in the repulsive region to overlap, which results in a transition transfer of electrons [56]. Notably, from the principle of power generation, the requirements for triboelectricity generation are considerably broader compared with piezoelectric materials. Merely the difference in triboelectric polarity between two contacting objects is sufficient. Even identical materials that are subjected to varying degrees of curvature or surface treatment before contact manifest triboelectric effects [12]. Additionally, triboelectricity outperforms piezoelectricity in terms of power generation capacity by yielding a higher voltage output at lower frequencies [57,58].

TENGs operate through five fundamental modes: contact–separation, lateral sliding, single electrode, independent layer, and rolling mode [59–62]. Each mode boasts distinct advantages in energy collection range, conversion efficiency, preparation techniques, device structure, and application versatility. The wider selection of materials and working modes and the lighter structural design provide advantages for TENGs in flexible device applications. To enhance the performance output, researchers employ dual strategies. On the one hand,

they augment the difference in electron binding ability within the contact layer by engineering various composite materials or introducing charge-gaining groups to facilitate charge transfer [63–65]. Moreover, they bolster the charge output by expanding the charge capture layer to mitigate charge recombination [66]. On the other hand, they optimize energy conversion efficiency by exploring diverse device structures, such as disk [67,68], zigzag [69], or fiber configurations [58]. Additionally, researchers enhanced the contact surface roughness through advanced surface treatments to maximize the contact area [70]. The recent progress in flexible triboelectric sensors is comprehensively summarized by focusing on two pivotal aspects: material advancements and innovative device structures. This dual-pronged approach ensures a holistic understanding of the evolving landscape in flexible triboelectric sensor technology, which offers insights into both material innovations and structural optimizations. A wider selection of materials and more diverse structural designs also provide a broader platform for TENG applications in self-powered flexible electronic devices [71,72].

3.1. Material Progress

Tremendous advancements have been made in the development of materials for TENGs, which is a pivotal technology in power generation. Despite the absence of stringent material constraints within TENG design, researchers persist in the quest for superior functional materials capable of delivering heightened performance and consistent output signals. This endeavor is approached through the exploration of composite materials and material modification strategies [73–75]. MXene nanosheets have a highly electronegative surface and electrical conductivity, which are not only easy to functionalize with functional groups but also easy to process into various complex shapes, and thus, they are widely used in flexible TENGs. Fan et al. made flexible electrodes by soaking cotton fabric in a mixed suspension of Ti_3C_2 MXene and cellulose nanofibers [76]. Leveraging electrostatic adsorption, MXene endows the electrodes with the requisite electrical conductivity and electronegativity. These electrodes, which are complemented by a silicone rubber friction layer and encapsulation material, facilitate the generation of voltages that reach up to 400 V under periodic palm pressure stimulation (Figure 6a). Additionally, the resulting TENG exhibits commendable mechanical robustness and linear pressure-sensing capabilities, which qualifies it for deployment as a self-powered flexible sensor for monitoring human physiological activities. Polyimide (PI) emerged as another promising material candidate for flexible TENG applications, owing to its outstanding thermal stability and flexibility. Li et al. pioneered the integration of PI into TENGs as a negatively charged component, thus culminating in the development of a self-healing PI-based TENG [77]. This innovation is realized through the incorporation of disulfide bonds and PDMS into the primary PI chain. The dynamic exchange reactions facilitated by the disulfide bonds confer upon PI the remarkable ability to self-heal, while the introduction of flexible PDMS serves to mitigate the rigidity of the PI chain and facilitates its molecular chain movement (Figure 6b). A self-healing TENG can basically return to the output level before damage after a fitting repair. It is worth noting that due to the presence of CF_3 electron-absorbing groups and siloxane fragments in the composite PI film, the output performance of the composite PI film is also twice that of the ordinary PI-based TENG, which underscores the efficacy of such strategic material modifications in advancing TENG technology.

The utilization of 2D materials in flexible TENG represents a burgeoning frontier in electronic functional materials, owing to their exceptional electrical properties, flexibility, high specific surface area, and tunable band gap [78,79]. These materials serve not only as effective frictional agents for generating transfer charge but also as promising fillers within polymer matrices for doping and modification purposes [80]. Notably, Xia et al. developed a flexible TENG that employed AGS@PDMS, wherein graphene nanosheets were embedded within a PDMS matrix through a process of repeated spin coating (SC) [81]. This technique facilitates the precise alignment of two-dimensional aligned graphene sheets (AGSs) parallel to the PDMS surface, which effectively creating numerous micro-capacitors within the material (Figure 6c). Consequently, this arrangement enhances the device's overall capacitance and dielectric loss while concurrently augmenting the frictional charge

accumulation on the PDMS surface. Comparative analyses demonstrate that TENGs fabricated using this SC methodology outperformed those produced via conventional spin-coating techniques by showcasing superior properties over pure PDMS-based TENGs. In a seminal contribution, Wu et al. pioneered the incorporation of reduced graphene oxide (rGO) into polyimide (PI) films as frictional agents [82]. Through fluorescence and absorption spectroscopy analyses, it was observed that rGO possesses a remarkable capability to capture non-volatile electrons, thereby mitigating charge recombination and facilitating charge transfer (Figure 6d). The integration of rGO resulted in significant enhancements in TENG performance, with TENGs employing PI (Kapton)/PI:rGO/PI configurations that achieved a remarkable maximum output voltage (190 V) and power (6.3 Wm^{-2}). Furthermore, Yang et al. elucidated that the uniform dispersion of graphene within polymer matrices yields a graphene-rich transfer film on friction surfaces, thereby lubricating the interface and prolonging the device's lifespan [83]. This multifaceted approach underscores the pivotal role of 2D materials in advancing the performance and functionality of flexible TENGs, thus offering promising avenues for future research and development in energy harvesting and related fields.

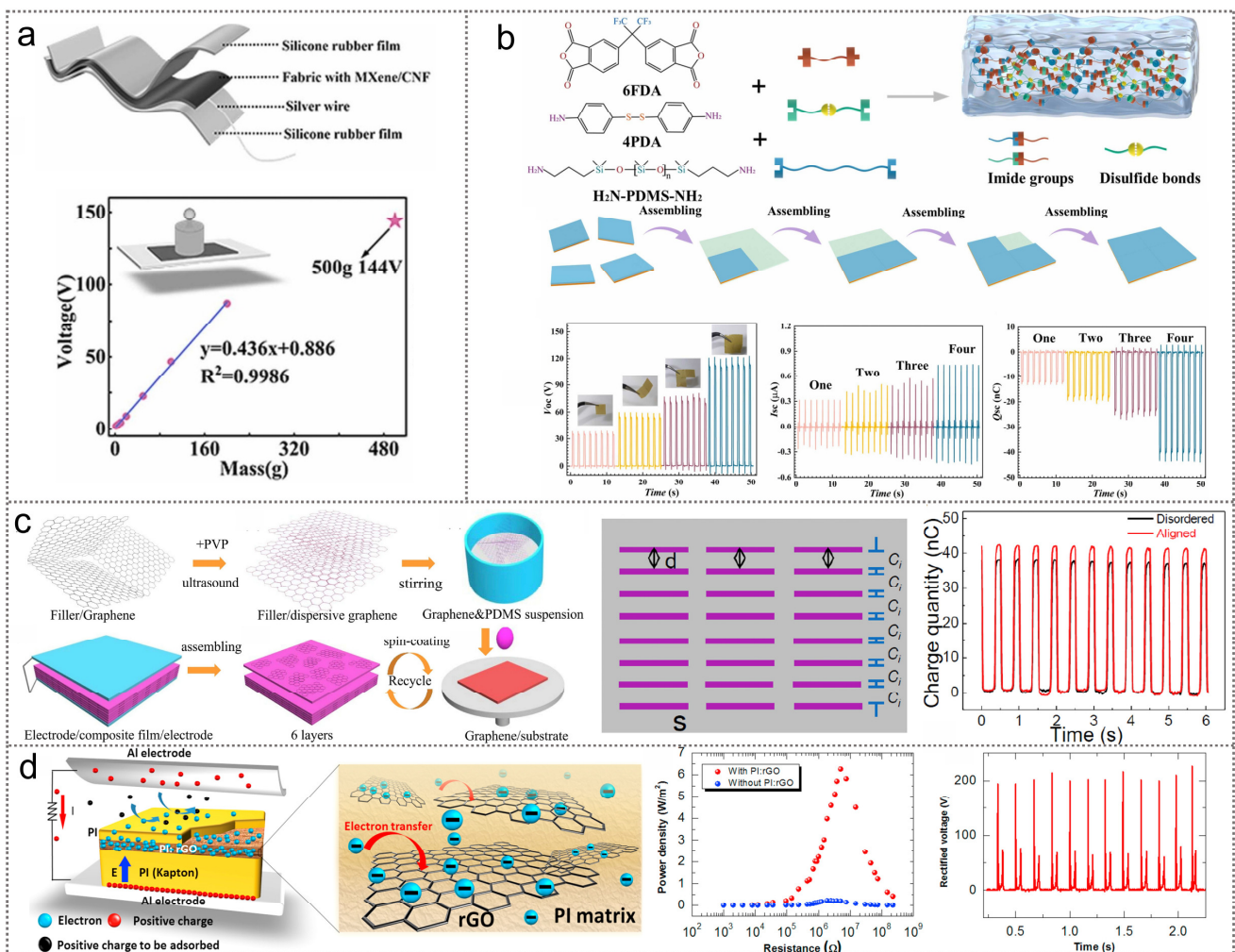


Figure 6. Progress of flexible TENGs in materials. (a) The flexible electrode for a TENG was prepared by soaking cotton fabric in a mixed suspension of Ti_3C_2 and cellulose nanofibers. Reprinted with permission from Ref. [76]. Copyright 2023, Elsevier. (b) Self-healing TENG based on a composite PI membrane. Reprinted with permission from Ref. [77]. Copyright 2023, Elsevier. (c) High-performance flexible TENG based on AGS@PDMS. Reprinted with permission from Ref. [81]. Copyright 2016, Elsevier. (d) rGO was incorporated into PI as an electron-trapping layer. Reprinted with permission from Ref. [82]. Copyright 2017, Elsevier.

3.2. Structural Progress

Structural optimization stands as a pivotal strategy for enhancing the efficacy of flexible TENGs. Among the myriad approaches, surface modification of the friction layer material emerges as a direct and effective means, which facilitates the creation of a textured surface. This surface roughness serves to augment the frictional area, thereby bolstering the charge transfer and, consequently, the output performance of TENGs. In a seminal study, Park et al. elucidated the fabrication of a two-dimensional MoS₂ thin layer from (NH₄)₂MoS₄ on a SiO₂ substrate through laser directional annealing [84]. By adeptly controlling the laser power, the ensuing thermal stress induced a separation between the SiO₂ thin layer and the Si substrate, which leads to the formation of interfacial cavities and diverse folding structures. These folded MoS₂ configurations serve a dual role: first, they amplify the contact surface area for friction, and second, they engender lattice stretching, thereby elevating the work function and enhancing electron attraction, which collectively facilitates an improved charge transfer efficiency (Figure 7a). Cai et al. innovatively constructed a flexible TENG self-powered tactile sensor predicated on a folded PDMS/MXene composite film that was synthesized via ultraviolet ozone (UVO) irradiation [85]. Upon exposure to UVO, the PDMS undergoes a transformative process, whereby the soft elastomeric surface transitions into a rigid silicon-like layer. The subsequent release of tension results in surface folding due to a mechanical mismatch, as the underlying PDMS remains untreated and exhibits normal recovery. Furthermore, the UVO treatment induces the conversion of –CH₃ groups to –OH, thereby augmenting the presence of oxygen-containing functional groups and facilitating enhanced electron adsorption (Figure 7b). This intricate interplay of structural modification and chemical functionalization culminates in heightened triboelectric properties and pressure sensitivity, thus rendering the sensor adept at capturing an array of physiological activities, including breathing, heartbeat, and muscle contraction.

On the other hand, the diverse operational modes inherent to TENGs serve as a versatile framework for researchers to enhance triboelectric properties through structural innovation. Wang et al. pioneered a novel variable charge density–single electrode configuration that capitalizes on the principle that charge density fluctuates with the relative stretching of the friction layer post-contact [19]. Employing polyethylene (PE) and silicone rubber as the frictional interface, the stretching of silicone rubber induces a decline in the surface negative charge density, thereby elevating the potential of the PE layer and facilitating the migration of electrons toward the electrode (Figure 7c). Furthermore, the sensor is directly applicable for tactile sensing in a vertical contact–separation mode. In a bid to address the limited detection range inherent to TENGs, Xu devised a wide-range triboelectric pressure sensor featuring a double sandwich structure integrating two distinct friction layers with varying Young's moduli [86]. PDMS and silicone rubber, which are characterized by differing deformations under distinct pressure ranges, alternately dominate and are augmented by the incorporation of cylinders featuring diverse inclination angles on their surfaces. This design optimization yields heightened sensitivity across a broad spectrum of pressures, ranging from 8.72 Pa to 450 kPa. Furthermore, through the integration of this self-powered pressure sensor with a deep learning model, a robust human motion recognition system predicated on plantar pressure is engineered, which boasts an impressive accuracy rate of 99.42% (Figure 7d).

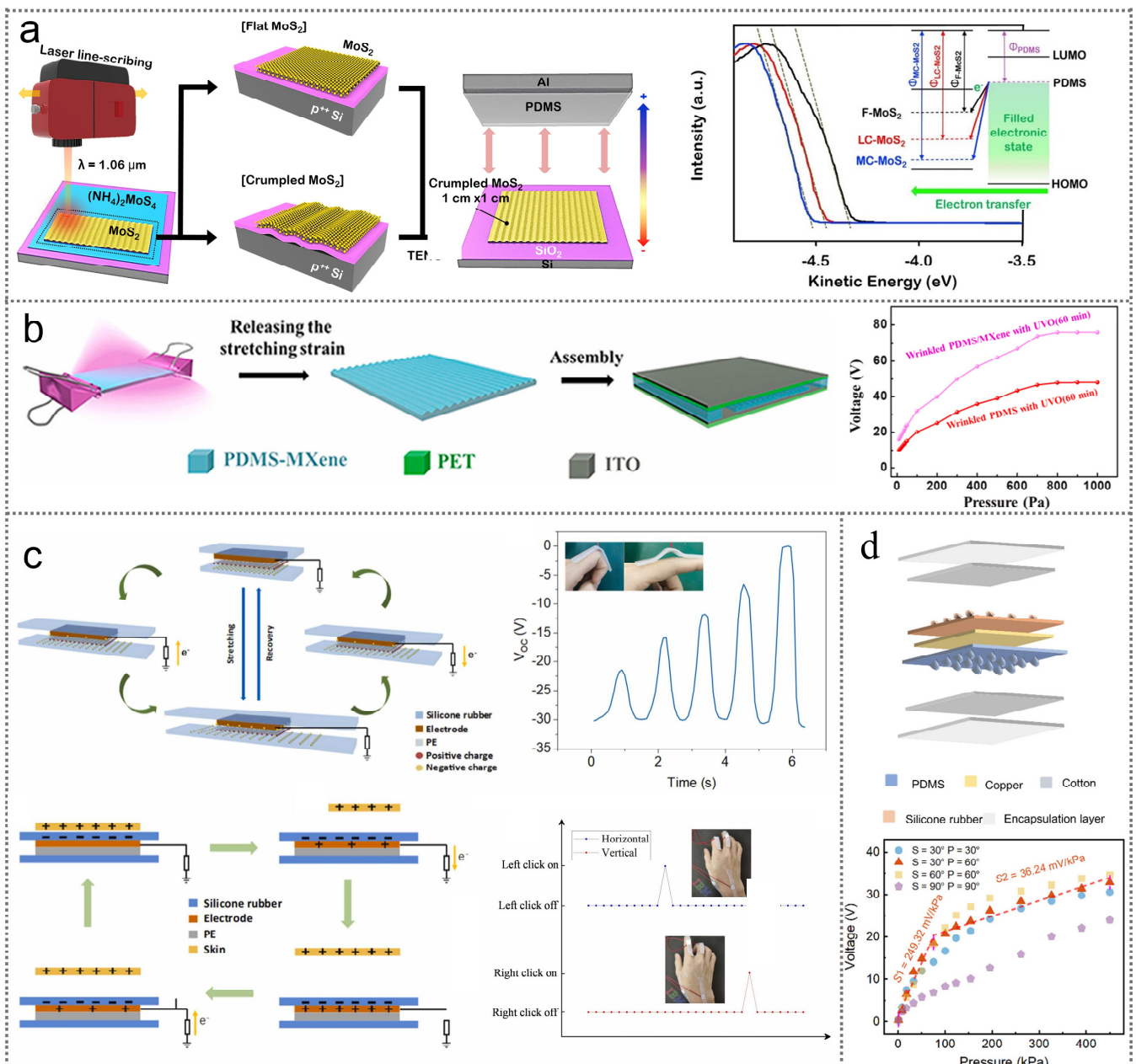


Figure 7. Progress of flexible TENGs in structural design. (a) Laser-induced folding MoS₂ as the friction layer of a TENG. Reprinted with permission from Ref. [84]. Copyright 2020, Elsevier. (b) UVO treatment prestretching PDMS-MXene produces wrinkled surfaces. Reprinted with permission from Ref. [85]. Copyright 2021, Elsevier. (c) Strain–pressure dual mode self-powered sensor based on variable charge density–single electrode mode. Reprinted with permission from Ref. [19]. Copyright 2024, Elsevier. (d) Double sandwich structure based on friction materials with different Young’s modulus enhances the working range of TENG sensors. Reprinted with permission from Ref. [86]. Copyright 2022, American Chemical Society.

4. Flexible Pyroelectric Sensor

The pyroelectric effect was initially observed within the context of investigating the influence of temperature on material polarization intensity. As time went on, the trajectory of research on pyroelectric materials and their applications has been significantly propelled forward by the advent of laser and infrared technologies, thus rendering it a focal point of scientific inquiry [87,88]. The pyroelectric effect ensues from fluctuations in the surface charge density of a material under the sway of external temperature variations with time.

Beyond the intrinsic asymmetry inherent in the lattice structure of piezoelectric materials, pyroelectric substances necessitate self-polarization to engender an electric field within the crystal lattice. Consequently, alterations in external temperature precipitate shifts in the electric dipole moment centers within the material, thereby effectuating changes and the transference of a surface-bound charge [89]. Pyroelectric materials exhibit diverse structural compositions that are broadly classified into single-crystal materials (LiNbO₃, ZnO), metal oxide ceramics (PZT), organic polymers (PVDF), and composite materials [90–92].

Notably, contemporary research underscores the striking similarity in material selection between pyroelectric and piezoelectric sensors, with both predominantly relying on ferroelectric materials to optimize performance regulation and electrical output. Furthermore, the pursuit of flexible pyroelectric materials presents analogous challenges to those encountered in the development of flexible piezoelectric counterparts, notably concerning the harmonization of pyroelectric properties, flexibility, and fabrication techniques. Thus, aligned with this principle, researchers persist in enhancing the performance of flexible pyroelectric nanogenerators (PyENGs) through meticulous material modification and the refinement of preparation processes [87]. However, it is pertinent to underscore that the operational range of pyroelectric devices is inherently constrained by the Curie temperature of the constituent material, which is important to consider such that these devices function within variable temperature environments. Recent advancements in the realm of flexible pyroelectric sensors have been characterized by innovations in material modification and preparation techniques, which is a discourse that we shall elaborate upon in delineating recent research progress.

4.1. Material Modification

The enhancement of pyroelectric materials parallels that of piezoelectric materials, which was often achieved through the manipulation of crystallinity, strain coupling effects, and other techniques to augment the material's intrinsic polarization strength [91]. For instance, lead methyl iodide (CH₃NH₃PbI₃) (MAPI) exhibits notable infrared activity. Sultana mixed it into PVDF to prepare a piezoelectric pyroelectric nanogenerator (P-PNG) by electrospinning [93]. The addition of MAPI particles enhanced the charge density in the electrospinning solution, which resulted in an increase in the exerting force in the jet, and thus, increased the yield of polar β in the PVDF. A comparative analysis revealed that PVDF-MAPI composites boasted an electroactive phase fraction of 95% and was accompanied by a pyroelectric coefficient of approximately 44 pC/m² K, alongside rapid response and reset times (Figure 8a). Similarly, Gupta et al. employed electrospinning techniques to incorporate MXene nanosheets into PVDF nanofibers, thereby enhancing the surface properties of the resulting composite [20]. This integration not only augmented the surface energy and surface potential but also facilitated the formation of favorable out-of-plane dipole arrangements within the composite structure (Figure 8b). The constrained effect of two-dimensional MXene nanosheets significantly bolstered the pyroelectric response of the composite fibers, thus yielding a remarkable pyroelectric coefficient of 130 nC/m² K. Moreover, leveraging this high-performance flexible pyroelectric material, the researchers successfully implemented it in breath and proximity sensors. Integration with machine learning algorithms further facilitated advanced data analysis techniques.

Wu et al. devised a method for fabricating a self-polarized PVDF film through the hydrophilic treatment of a glass substrate [94]. This treatment induces the formation of hydroxyl groups on the glass surface. Upon depositing the PVDF solution, the electronegativity disparity between fluorine and hydrogen atoms leads to the establishment of hydrogen bonds (Figure 8c). These bonds organize themselves into a subnanometer-thick layer in an orderly fashion and serve as a seed layer that catalyzes the subsequent alignment of the PVDF solution, thereby facilitating self-polarization. Experimental findings revealed that the β -phase content post-surface treatment exhibited a significant enhancement of 50% compared with the initial sample. Furthermore, to mitigate the piezoelectric interference inherent in pyroelectric sensor operation, the researchers developed a novel double-layer pyroelectric sensor by employing the aforementioned PVDF film. Notably, a PDMS cylinder

was interposed between the two layers of PVDF, thus fulfilling the dual role of thermal insulation and vibration transmission. Comparative analysis demonstrated a substantial enhancement in the signal-to-noise ratio of the double-layer configuration, which elevated it from 18 dB to 38 dB and surpassed that of the single-layer sensor.

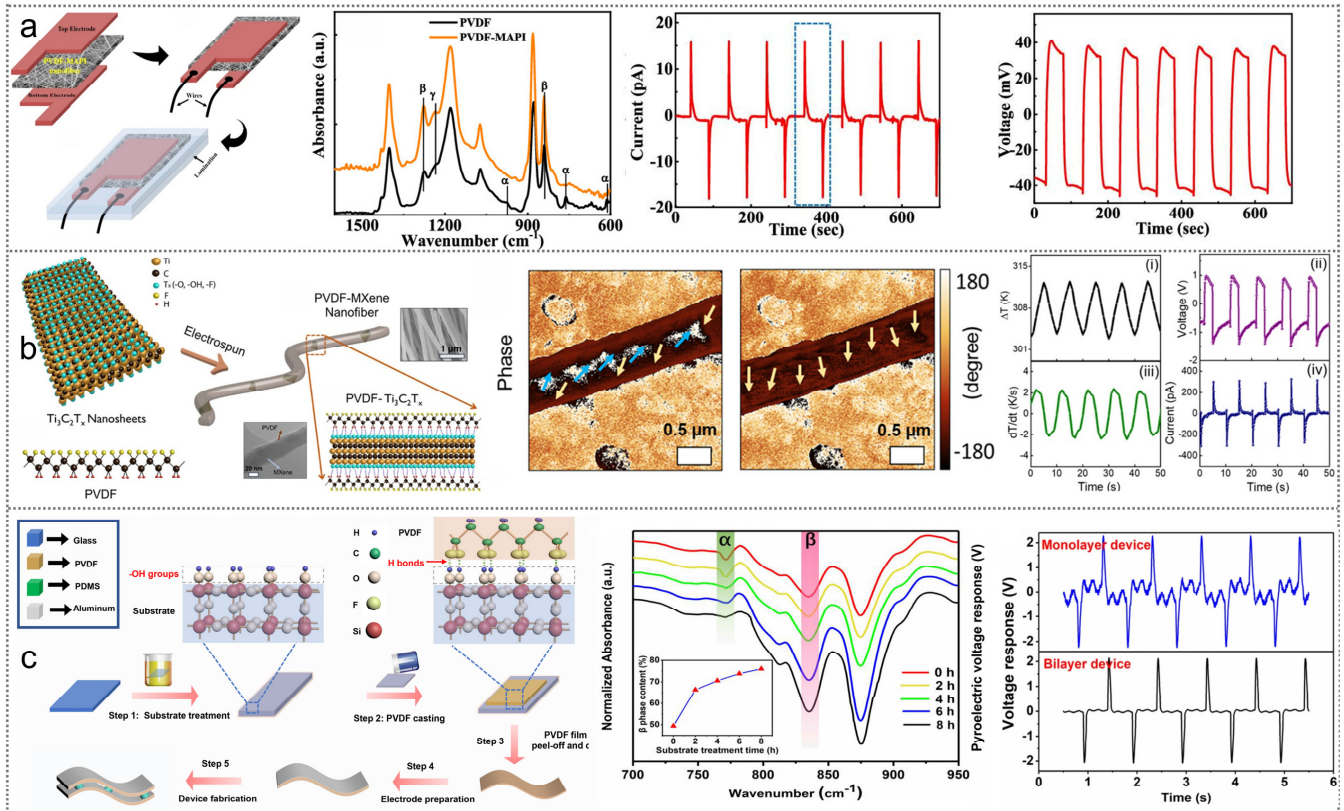


Figure 8. Progress in the material modification of flexible PyNG. (a) MAPI was incorporated into PVDF to enhance the yield of the polar β phase. Reprinted with permission from Ref. [93]. Copyright 2019, American Chemical Society. (b) The pyroelectric response of PVDF fibers was enhanced by the confinement of two-dimensional MXene nanosheets. (i) to (iv) show temperature input changes and corresponding temperature responses, respectively. Reprinted with permission from Ref. [20]. Copyright 2024, American Chemical Society. (c) Hydrophilic substrate promotes PVDF spontaneous polarization [94].

4.2. Progress in Preparation Technology

Researchers are exploring various avenues to enhance the performance of thermal release band sensors, not only by refining the properties of thermal functional materials but also by optimizing the device preparation process, device structure, and radiation absorption capabilities. One notable approach involves the improvement of electrode materials. Lee et al. investigated the integration of tosylate into PEDOT:TOS to create a highly efficient thermal radiation absorption electrode for PVDF [95]. This strategy aimed to mitigate the reflection of thermal radiation commonly encountered with conventional metal materials. PEDOT:TOS demonstrates a broad thermal radiation absorption band. Through experimentation with different preparation methods, the researchers observed that PEDOT:TOS electrodes, when prepared via oven heating, exhibited an increased thickness, a rougher surface, and a porous morphology (Figure 9a). These characteristics expedite the thermally induced polarization changes in the PVDF and augment the charge released on the electrode surface. Comparative analyses with metal and other organic electrodes revealed a significant enhancement in the thermoelectric conversion efficiency, which surpassed previous benchmarks by several folds or even an order of magnitude. In a separate study, Guan et al. explored the incorporation of microstructures within PVDF films to enhance their pyroelectric response [96]. By depositing

precursor solutions onto templates featuring groove, square pit, and sine patterns, PVDF films with diverse structures were fabricated (Figure 9b). The researchers observed that the presence of microstructure patterns, particularly the increased sidewall surface area, led to the generation of additional heat flow components upon exposure to thermal radiation. Consequently, this enhanced the pyroelectric response of the PVDF film by up to 146% compared with flat surfaces. Further analysis through simulation underscored the critical influence of the surface topology, sidewall angles, and pattern width on the film’s responsiveness, indicating avenues for tailored optimization in future research endeavors.

Fattori introduced a novel approach by integrating printed P(VDF-TrFE) thin-film pyroelectric sensors with OTFT integrated circuits, thus facilitating the creation of a flexible large-area proximity sensing surface [21]. The OTFT array serves as an active front-end electronics (AFE) device that offers signal amplification, enhanced immunity to external interference, and the mitigation of pixel crosstalk through pixel addressing (Figure 9c). Moreover, the pyroelectric sensor is configured to operate in current mode, which is facilitated by a dedicated OTFT current sense amplifier and multiplexing scheme employing time-division methods. This configuration allows for adequate signal amplification while reducing the transistor count complexity, thus improving the overall circuit yield. Notably, this implementation marks the largest circuit realized by a printed OTFT circuit. The AFE, in conjunction with the pyroelectric sensor, achieved a power sensitivity of $267 \text{ nW Hz}^{-1/2}$ at a power consumption level of $54 \text{ }\mu\text{W}$. Additionally, the incorporation of 3D-printed infrared guided funnel arrays enhances the directional sensitivity of individual sensors, thus further refining the detection capabilities of the system.

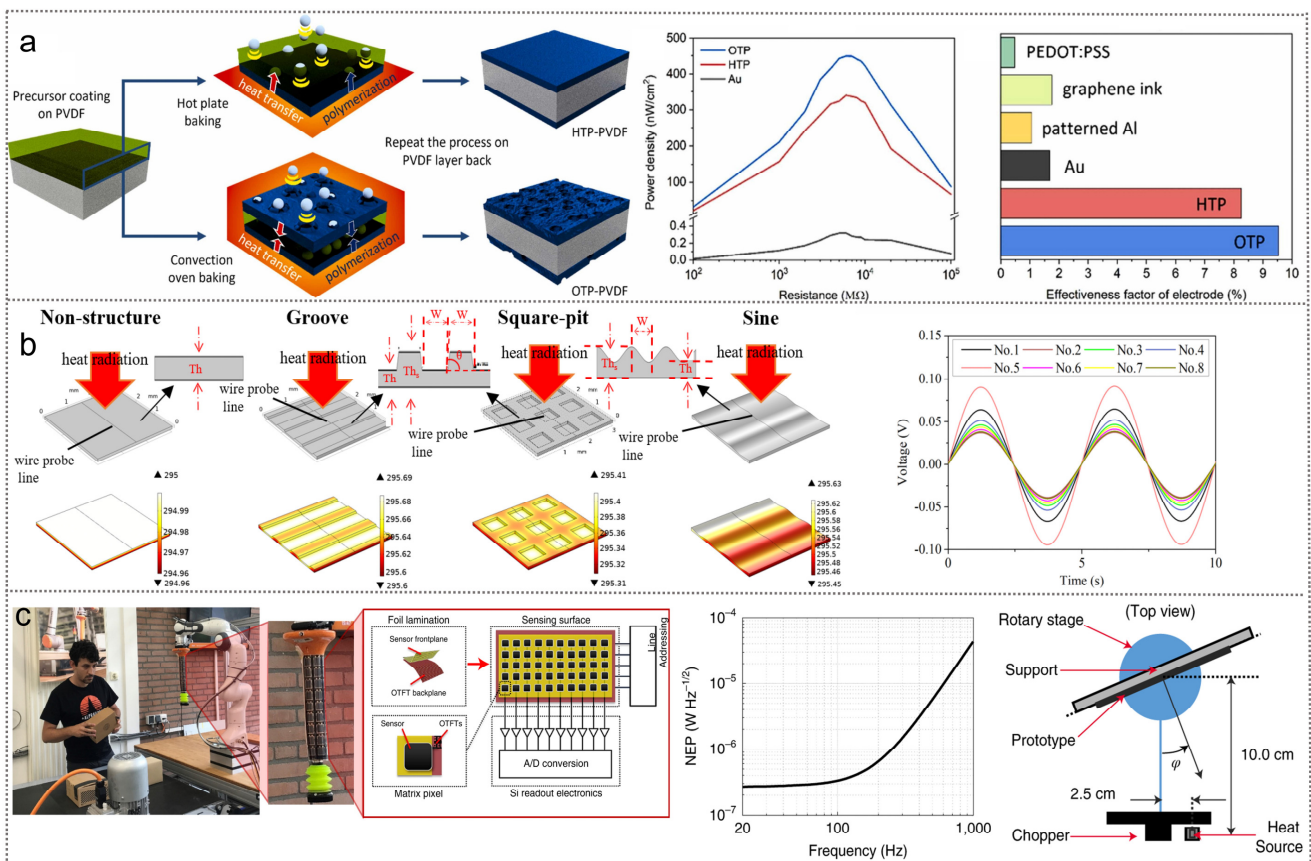


Figure 9. Progress in preparation technology of flexible PyNG. (a) High-efficiency thermal-radiation-absorbing electrode was prepared by regulating PEDOT:TOS growth conditions. Reprinted with permission from Ref. [95]. Copyright 2022, Elsevier. (b) Pyroelectric response of PVDF thermal films with different microstructures [96]. (c) P(VDF-TrFE) is combined with OTFT array to prepare flexible large area proximity sensing surface [21].

5. Hybrid Generation Mode

The preceding discussion delves into the research advancements concerning three primary flexible nanogenerators and their accompanying sensors, which encompasses pressure, friction, and thermal power generation. These sensors demonstrate the capability to detect a range of stimuli, including external pressure, bending, friction, and temperature fluctuations. Table 1 summarizes the comparison of the three sensors in terms of their material selection, power generation performance, advantages, and disadvantages. Notably, researchers have primarily focused their efforts on refining equipment through enhancements in functional materials, preparation processes, and device structures, all of which are aimed at attaining heightened output quality. Despite these strides, achieving multifunctional sensing within a unified architecture remains a notable trend and challenge for flexible sensors [97]. The development of tactile sensors based on multiple power generation modes to achieve multifunctional sensing is also a reliable solution [15,98].

Table 1. Comparison of three power generation modes in terms of their material selection, power generation performance, advantages, and disadvantages.

Category	Materials	Electricity Generation Performance	Advantages	Disadvantages
PENG	Organic materials: PVDF and its copolymers, as well as piezoelectric biomaterials	The d_{33} value is generally around tens of pC/N	Intrinsic flexibility and easy doping modification	Weak piezoelectric response and high polarization voltage
	Inorganic materials: ZnO, perovskite ceramics, two-dimensional materials, and so on	The d_{33} value is generally around hundreds of pC/N	High and stable piezoelectric output	High hardness and resistance to bending
	Composite piezoelectric materials	The piezoelectric response is intermediate between organic and inorganic materials	With both flexible and high-voltage output	Complex preparation process
TENG	Materials with triboelectric polarity differences that match each other: MXene, PTFE, graphene and its derivatives, two-dimensional materials, and so on	The output voltage can reach hundreds to thousands of volts	High output voltage, low material requirements, and simple preparation	It is susceptible to environmental factors such as temperature, humidity, and impact; wear causes a reduction in its service life
PyNG	Similar to the materials used in piezoelectric devices, most of them are ferroelectric	The pyroelectric coefficient of organic pyroelectric materials is generally in the tens of $\mu\text{C}/(\text{m}^2\text{K})$, while that of inorganic pyroelectric materials is typically in the hundreds or even thousands of $\mu\text{C}/(\text{m}^2\text{K})$	It can be used for applications such as temperature sensing, ultraviolet/infrared light detection, and thermal imaging	The temperature response range of the devices is relatively low or narrow, the microscopic mechanism of the pyroelectric effect is insufficiently studied, and it has received limited attention

Composite power generation mode exemplifies the innovative integration of multiple energy-harvesting mechanisms within a singular device, specifically amalgamating principles from piezoelectricity, triboelectricity, and pyroelectricity. This multifaceted approach boasts discernible advantages over single-mode power generation systems. Leveraging multiple energy sources, composite power generation apparatuses demonstrate heightened efficiency and reliability, thus ensuring a consistent and robust power supply [13]. Furthermore, this integration affords a broader environmental adaptability, which allows the device to concurrently or sequentially perceive various external stimuli [14]. Consequently, self-powered sensors equipped with composite power generation modes herald a promising shift toward more versatile and efficient energy harvesting solutions.

The utilization of materials exhibiting piezoelectric and pyroelectric properties has garnered significant attention, with researchers endeavoring to leverage their overlapping characteristics for sensor development within the composite power generation mode. Roy et al. pioneered the creation of a piezoelectric/pyroelectric hybrid nanogenerator by uti-

lizing PVDF/GO composite nanofibers [99]. The incorporation of graphene oxide within the PVDF matrix facilitates stable nucleation of the PVDF- β phase, which enhances the piezoelectric and pyroelectric responses (Figure 10a). Moreover, graphene oxide's mid-infrared radiation absorption and efficient thermal conductivity within the fibers further augment sensor performance. This innovative approach yields impressive power densities of 6.2 mW/m^2 and 1.2 nW/m^2 for pressure and temperature changes, respectively. Notably, the sensor exhibits high sensitivity to finger, wrist, and elbow bending, along with temperature variations during respiration. Similarly, Shin et al. introduced a triboelectric/pyroelectric multimode pressure and temperature sensor based on P(VDF-TrFE) [98]. Through the opposite ferroelectric polarization of identical P(VDF-TrFE) materials, the contact material demonstrates substantially enhanced triboelectric and pyroelectric output properties. Noteworthy pressure sensitivities of up to 40 nA kPa^{-1} and sensitivity to heating and cooling of $0.38 \text{ nA}^\circ\text{C}^{-1}$ and $0.27 \text{ nA}^\circ\text{C}^{-1}$ were achieved. Employing distinct voltage and current responses under varying temperature conditions, the sensor effectively decouples pressure and temperature signals using the divergent responses and saturation times of the triboelectric and pyroelectric effects (Figure 10b). This novel preparation method and unique sensor structure hold promise for applications ranging from monitoring weak carotid pulse pressure to multimodal finger touch sensing.

Ma et al. devised a self-powered flexible antibacterial tactile sensor by leveraging the triboelectric properties of PTFE and the piezoelectric and pyroelectric properties of PVDF [15]. This innovative design facilitates multimodal sensing of both temperature and pressure. A graphene electrode serves as a common electrode for both PTFE and PVDF, thus enabling efficient coupling of their respective sensing mechanisms (Figure 10c). Moreover, the incorporation of silver nanowires into PTFE imparts antibacterial properties to the sensor. By exploiting the similar surface charge changes induced by pressure on PTFE and the piezoelectric effect of PVDF, the sensor achieves enhanced pressure sensing through the coupling of triboelectric and piezoelectric effects. The sensor exhibits monitoring sensitivities of 0.092 V/kPa for pressure and $0.11 \text{ V}/^\circ\text{C}$ for temperature. Furthermore, the decoupling of pressure and temperature signals is facilitated by the disparate response times of the triboelectric and pyroelectric effects. In addition to its primary sensing capabilities, the sensor enables real-time surface monitoring. These attributes render it highly promising for applications in electronic skin, artificial prosthetics, health monitoring, and beyond.

Pyroelectric signals can be distinguished by the difference in response time between piezoelectric/triboelectric and pyroelectric signals. However, the distinction between piezoelectric and triboelectric signals is easily ignored when testing the performance of piezoelectric and pyroelectric materials and composite power generation modes. Traditional testing methods often overlook the subtle disparity between piezoelectric and triboelectric signals due to their nearly synchronous generation times and similar output characteristics. Addressing this issue, Chen et al. devised an innovative approach to disentangle piezoelectric components from ostensibly "piezoelectric" signals [100]. Their method involves augmenting a PVDF-based self-powered sensor with a charge-shielding layer and scrutinizing the stress process curve. During the contact-compression-release-separation sequence, electrical signals preceding and following contact primarily reflect triboelectric contributions, whereas the signals post-contact predominantly stem from piezoelectric effects (Figure 10d). Leveraging this temporal discrepancy, the inflection points of these distinct electrical signals are successfully delineated in the pressure response curve through manipulation of the reverse of the piezoelectric signal and the friction signal. This methodological advancement facilitates a nuanced comparison of the piezoelectric and triboelectric properties of materials, thereby fostering the advancement of high-performance piezoelectric materials for wearable electronics applications. Such meticulous analysis not only enhances our understanding of material behavior but also propels the development of the next generation of wearable technologies.

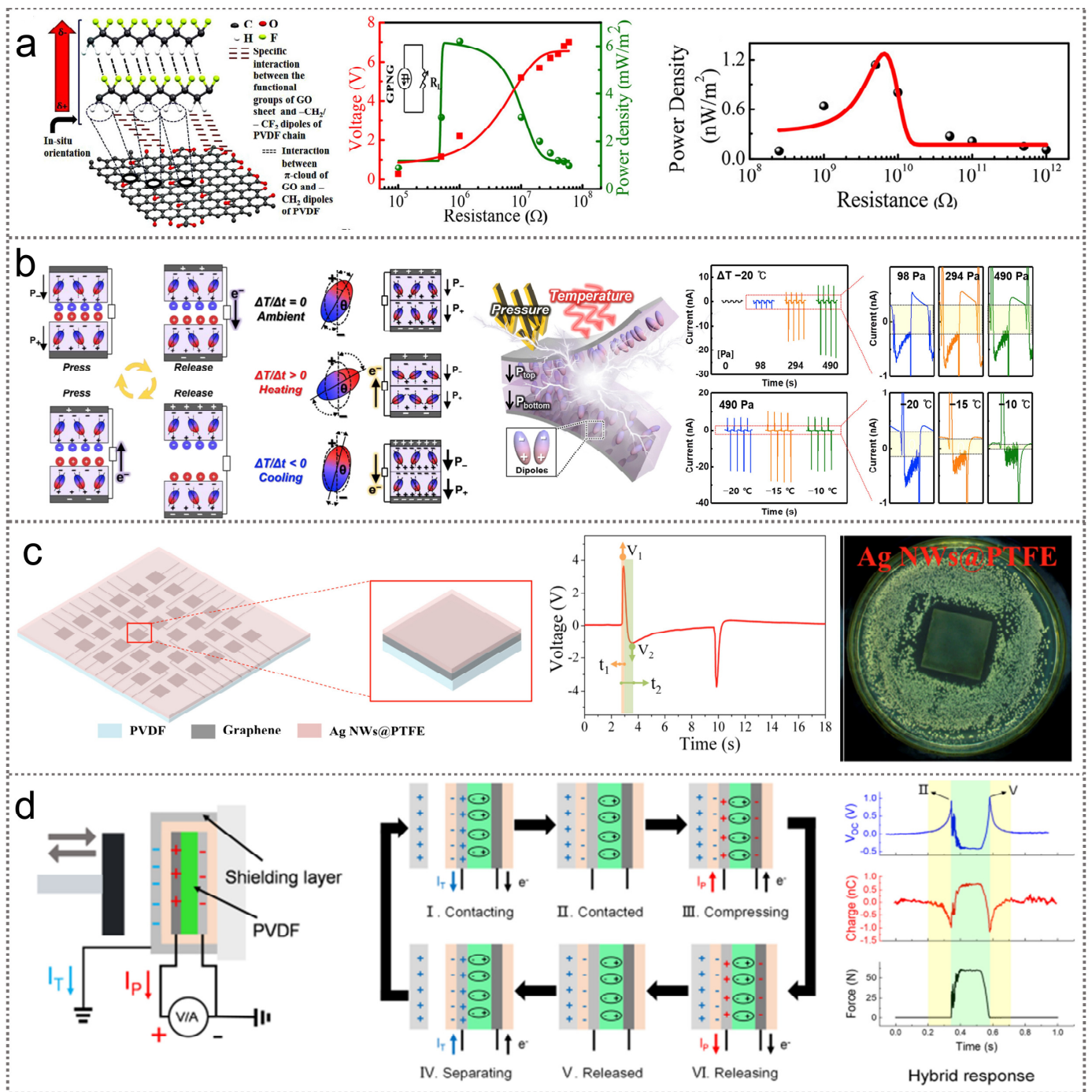


Figure 10. Research progress based on multiple power generation modes. (a) Piezoelectric/pyroelectric hybrid nanogenerator was designed using PVDF/GO composite nanofibers. Reprinted with permission from Ref. [99]. Copyright 2019, American Chemical Society. (b) Triboelectric/pyroelectric hybrid nanogenerator was designed based on P(VDF-TrFE) opposite ferroelectric polarization. Reprinted with permission from Ref. [98]. Copyright 2020, Elsevier. (c) Self-powered triboelectric/pyroelectric multimodal sensors with enhanced performances and decoupled multiple stimuli. Reprinted with permission from Ref. [15]. Copyright 2019, Elsevier. (d) A method for effectively distinguishing piezoelectric signals from triboelectric signals in a composite signal [100].

6. Summary and Outlook

This review summarizes and discusses three main self-powered modes, namely, PENG, TENG, and PyENG; composite generation; and the research progress of flexible sensors

based on them. It is not difficult to see that researchers are committed to innovation from functional materials; preparation processes and device structures to obtain higher and more stable output; and trying to use them for applications in the context of the Internet of things, such as human physiological monitoring and waste energy collection. However, there is still a gap between these self-powered sensors studied at present and their actual application.

First of all, for different kinds of energy generation modes, each face different problems. For example, for the ferroelectric materials used by PENGs and PyENGs, how to effectively combine the flexibility of organic materials with the characteristics of the high charge output of inorganic materials, as well as design functional materials with “fine and flexible combination” by means of material modification or process improvement, is still the primary problem in preparing flexible sensors for practical production applications. Directly, research into piezoelectric sensors should pay attention to the effects of temperature changes in the environment. Pyroelectric sensors also need to pay extra attention to the effective absorption of radiation and the range of working stations. For TENG-based flexible devices, although the material selection is less limited, it is still sensitive to ambient temperature, humidity, and mechanical vibration interference. In addition, the impact of damage to the contact material during friction contact on the service life of the device should also be paid attention to.

Second, for sensors with a composite power generation mode, although more signals can be collected for multi-mode sensing, decoupling the response made by different stimuli is also a limitation of its multi-mode sensing. Comprehensive use of the response time and output amplitude of different effects, as well as design of different response or output modes, are also common methods for other multi-mode sensor decoupling.

Finally, sensors based on different nanogenerators should not only be limited to sensing the outside world through the signal generated by their own power generation. With the development of wearable and implantable flexible devices, power supply issues, such as bulky, replaceable electrode modules or complex external wires, have an increasingly significant impact on the user experience. The intrinsic advantage of self-power should be integrated with other sensing modules, even wireless interconnection, information processing, and other modules, and the flexible electronic devices that are closer to actual references can be realized through optimized structural design and device interconnection.

In short, in the context of the development of the Internet of everything, flexible electronic devices show unique advantages in the fields of health detection, human–computer interaction, and so on. The energy supply modes represented by PENG, TENG, and PyENG propose additional solutions for energy collection and utilization, which not only provide a broader development platform for flexible sensors but also lead to the use of flexible electronic devices in more practical applications. It can be seen that through the innovation and improvement of the materials, preparation process, and device structure, self-powered technology will certainly promote flexible electronic devices to a higher level.

Author Contributions: Conceptualization, Y.Z., W.C. and L.P.; writing—original draft preparation, Y.Z.; review and editing, J.-H.Z., J.H. and F.W.; funding acquisition, L.P. and Y.S. All authors have read and agreed to the published version of the manuscript.

Funding: This work was supported by the National Key Research and Development Program of China under grant no. 2021YFA1401103 and the National Natural Science Foundation of China under grants 61825403, 61921005, and 61674078.

Data Availability Statement: No new data were created or analyzed in this study. Data sharing is not applicable to this article.

Conflicts of Interest: The authors declare no conflicts of interest.

References

1. Someya, T.; Bao, Z.; Malliaras, G.G. The Rise of Plastic Bioelectronics. *Nature* **2016**, *540*, 379–385. [[CrossRef](#)]
2. Lee, J.-H.; Cho, K.; Kim, J.-K. Age of Flexible Electronics: Emerging Trends in Soft Multifunctional Sensors. *Adv. Mater.* **2024**, *36*, 2310505. [[CrossRef](#)] [[PubMed](#)]
3. Hammock, M.L.; Chortos, A.; Tee, B.C.-K.; Tok, J.B.-H.; Bao, Z. 25th Anniversary Article: The Evolution of Electronic Skin (E-Skin): A Brief History, Design Considerations, and Recent Progress. *Adv. Mater.* **2013**, *25*, 5997–6038. [[CrossRef](#)] [[PubMed](#)]
4. Wang, M.; Luo, Y.; Wang, T.; Wan, C.; Pan, L.; Pan, S.; He, K.; Neo, A.; Chen, X. Artificial Skin Perception. *Adv. Mater.* **2021**, *33*, 2003014. [[CrossRef](#)] [[PubMed](#)]
5. Chen, W.; Yan, X. Progress in Achieving High-Performance Piezoresistive and Capacitive Flexible Pressure Sensors: A Review. *J. Mater. Sci. Technol.* **2020**, *43*, 175–188. [[CrossRef](#)]
6. Wang, S.; Xu, J.; Wang, W.; Wang, G.-J.N.; Rastak, R.; Molina-Lopez, F.; Chung, J.W.; Niu, S.; Feig, V.R.; Lopez, J.; et al. Skin Electronics from Scalable Fabrication of an Intrinsically Stretchable Transistor Array. *Nature* **2018**, *555*, 83–88. [[CrossRef](#)]
7. Cao, X.; Xiong, Y.; Sun, J.; Zhu, X.; Sun, Q.; Wang, Z.L. Piezoelectric Nanogenerators Derived Self-Powered Sensors for Multifunctional Applications and Artificial Intelligence. *Adv. Funct. Mater.* **2021**, *31*, 2102983. [[CrossRef](#)]
8. Deng, W.; Zhou, Y.; Libanori, A.; Chen, G.; Yang, W.; Chen, J. Piezoelectric Nanogenerators for Personalized Healthcare. *Chem. Soc. Rev.* **2022**, *51*, 3380–3435. [[CrossRef](#)]
9. Yang, Z.; Zhu, Z.; Chen, Z.; Liu, M.; Zhao, B.; Liu, Y.; Cheng, Z.; Wang, S.; Yang, W.; Yu, T. Recent Advances in Self-Powered Piezoelectric and Triboelectric Sensors: From Material and Structure Design to Frontier Applications of Artificial Intelligence. *Sensors* **2021**, *21*, 8422. [[CrossRef](#)]
10. Dong, K.; Wu, Z.; Deng, J.; Wang, A.C.; Zou, H.; Chen, C.; Hu, D.; Gu, B.; Sun, B.; Wang, Z.L. A Stretchable Yarn Embedded Triboelectric Nanogenerator as Electronic Skin for Biomechanical Energy Harvesting and Multifunctional Pressure Sensing. *Adv. Mater.* **2018**, *30*, 1804944. [[CrossRef](#)]
11. Nozariasbmarz, A.; Collins, H.; Dsouza, K.; Polash, M.H.; Hosseini, M.; Hyland, M.; Liu, J.; Malhotra, A.; Ortiz, F.M.; Mohaddes, F.; et al. Review of Wearable Thermolectric Energy Harvesting: From Body Temperature to Electronic Systems. *Appl. Energy* **2020**, *258*, 114069. [[CrossRef](#)]
12. Xu, C.; Zhang, B.; Wang, A.C.; Zou, H.; Liu, G.; Ding, W.; Wu, C.; Ma, M.; Feng, P.; Lin, Z.; et al. Contact-Electrification between Two Identical Materials: Curvature Effect. *ACS Nano* **2019**, *13*, 2034–2041. [[CrossRef](#)] [[PubMed](#)]
13. Zi, Y.; Lin, L.; Wang, J.; Wang, S.; Chen, J.; Fan, X.; Yang, P.-K.; Yi, F.; Wang, Z.L. Triboelectric–Pyroelectric–Piezoelectric Hybrid Cell for High-Efficiency Energy-Harvesting and Self-Powered Sensing. *Adv. Mater.* **2015**, *27*, 2340–2347. [[CrossRef](#)] [[PubMed](#)]
14. Kim, J.; Lee, J.H.; Ryu, H.; Lee, J.-H.; Khan, U.; Kim, H.; Kwak, S.S.; Kim, S.-W. High-Performance Piezoelectric, Pyroelectric, and Triboelectric Nanogenerators Based on P(VDF-TrFE) with Controlled Crystallinity and Dipole Alignment. *Adv. Funct. Mater.* **2017**, *27*, 1700702. [[CrossRef](#)]
15. Ma, M.; Zhang, Z.; Zhao, Z.; Liao, Q.; Kang, Z.; Gao, F.; Zhao, X.; Zhang, Y. Self-Powered Flexible Antibacterial Tactile Sensor Based on Triboelectric-Piezoelectric-Pyroelectric Multi-Effect Coupling Mechanism. *Nano Energy* **2019**, *66*, 104105. [[CrossRef](#)]
16. Chen, X.; Qin, H.; Qian, X.; Zhu, W.; Li, B.; Zhang, B.; Lu, W.; Li, R.; Zhang, S.; Zhu, L.; et al. Relaxor Ferroelectric Polymer Exhibits Ultrahigh Electromechanical Coupling at Low Electric Field. *Science* **2022**, *375*, 1418–1422. [[CrossRef](#)]
17. Li, J.; Carlos, C.; Zhou, H.; Sui, J.; Wang, Y.; Silva-Pedraza, Z.; Yang, F.; Dong, Y.; Zhang, Z.; Hacker, T.A.; et al. Stretchable Piezoelectric Biocrystal Thin Films. *Nat. Commun.* **2023**, *14*, 6562. [[CrossRef](#)]
18. Gao, X.; Zheng, M.; Yan, X.; Fu, J.; Zhu, M.; Hou, Y. The Alignment of BCZT Particles in PDMS Boosts the Sensitivity and Cycling Reliability of a Flexible Piezoelectric Touch Sensor. *J. Mater. Chem. C* **2019**, *7*, 961–967. [[CrossRef](#)]
19. Wang, L.; Wei, F.; Zhai, Z.; Zhang, R.; Liu, W.; Zhao, Z. A Flexible Dual-Mode Triboelectric Sensor for Strain and Tactile Sensing toward Human-Machine Interface Applications. *Sens. Actuators Phys.* **2024**, *365*, 114909. [[CrossRef](#)]
20. Gupta, V.; Mallick, Z.; Choudhury, A.; Mandal, D. On-Demand MXene-Coupled Pyroelectricity for Advanced Breathing Sensors and IR Data Receivers. *Langmuir* **2024**, *40*, 8897–8910. [[CrossRef](#)]
21. Fattori, M.; Cardarelli, S.; Fijn, J.; Harpe, P.; Charbonneau, M.; Locatelli, D.; Lombard, S.; Laugier, C.; Tournon, L.; Jacob, S.; et al. A Printed Proximity-Sensing Surface Based on Organic Pyroelectric Sensors and Organic Thin-Film Transistor Electronics. *Nat. Electron.* **2022**, *5*, 289–299. [[CrossRef](#)]
22. Wu, Y.; Ma, Y.; Zheng, H.; Ramakrishna, S. Piezoelectric Materials for Flexible and Wearable Electronics: A Review. *Mater. Des.* **2021**, *211*, 110164. [[CrossRef](#)]
23. Lu, L.; Ding, W.; Liu, J.; Yang, B. Flexible PVDF Based Piezoelectric Nanogenerators. *Nano Energy* **2020**, *78*, 105251. [[CrossRef](#)]
24. Mahapatra, S.D.; Mahapatra, P.C.; Aria, A.I.; Christie, G.; Mishra, Y.K.; Hofmann, S.; Thakur, V.K. Piezoelectric Materials for Energy Harvesting and Sensing Applications: Roadmap for Future Smart Materials. *Adv. Sci.* **2021**, *8*, 2100864. [[CrossRef](#)]
25. Fan, F.R.; Tang, W.; Wang, Z.L. Flexible Nanogenerators for Energy Harvesting and Self-Powered Electronics. *Adv. Mater.* **2016**, *28*, 4283–4305. [[CrossRef](#)]
26. Wang, Z.L.; Song, J. Piezoelectric Nanogenerators Based on Zinc Oxide Nanowire Arrays. *Science* **2006**, *312*, 242–246. [[CrossRef](#)] [[PubMed](#)]
27. Zhou, H.; Zhang, Y.; Qiu, Y.; Wu, H.; Qin, W.; Liao, Y.; Yu, Q.; Cheng, H. Stretchable Piezoelectric Energy Harvesters and Self-Powered Sensors for Wearable and Implantable Devices. *Biosens. Bioelectron.* **2020**, *168*, 112569. [[CrossRef](#)] [[PubMed](#)]

28. Wei, C.; Jing, X. A Comprehensive Review on Vibration Energy Harvesting: Modelling and Realization. *Renew. Sustain. Energy Rev.* **2017**, *74*, 1–18. [[CrossRef](#)]
29. Park, K.-I.; Jeong, C.K.; Kim, N.K.; Lee, K.J. Stretchable Piezoelectric Nanocomposite Generator. *Nano Converg.* **2016**, *3*, 12. [[CrossRef](#)] [[PubMed](#)]
30. Vijayakanth, T.; Liptrot, D.J.; Gazit, E.; Boomishankar, R.; Bowen, C.R. Recent Advances in Organic and Organic–Inorganic Hybrid Materials for Piezoelectric Mechanical Energy Harvesting. *Adv. Funct. Mater.* **2022**, *32*, 2109492. [[CrossRef](#)]
31. Guo, S.; Duan, X.; Xie, M.; Aw, K.C.; Xue, Q. Composites, Fabrication and Application of Polyvinylidene Fluoride for Flexible Electromechanical Devices: A Review. *Micromachines* **2020**, *11*, 1076. [[CrossRef](#)] [[PubMed](#)]
32. Wan, X.; Cong, H.; Jiang, G.; Liang, X.; Liu, L.; He, H. A Review on PVDF Nanofibers in Textiles for Flexible Piezoelectric Sensors. *ACS Appl. Nano Mater.* **2023**, *6*, 1522–1540. [[CrossRef](#)]
33. Yuan, X.; Yan, A.; Lai, Z.; Liu, Z.; Yu, Z.; Li, Z.; Cao, Y.; Dong, S. A Poling-Free PVDF Nanocomposite via Mechanically Directional Stress Field for Self-Powered Pressure Sensor Application. *Nano Energy* **2022**, *98*, 107340. [[CrossRef](#)]
34. Xu, Q.; Gao, X.; Zhao, S.; Liu, Y.-N.; Zhang, D.; Zhou, K.; Khanbareh, H.; Chen, W.; Zhang, Y.; Bowen, C. Construction of Bio-Piezoelectric Platforms: From Structures and Synthesis to Applications. *Adv. Mater.* **2021**, *33*, 2008452. [[CrossRef](#)]
35. Lan, L.; Ping, J.; Xiong, J.; Ying, Y. Sustainable Natural Bio-Origin Materials for Future Flexible Devices. *Adv. Sci.* **2022**, *9*, 2200560. [[CrossRef](#)]
36. Teng, C.P.; Tan, M.Y.; Toh, J.P.W.; Lim, Q.F.; Wang, X.; Ponsford, D.; Lin, E.M.J.; Thitsartarn, W.; Tee, S.Y. Advances in Cellulose-Based Composites for Energy Applications. *Materials* **2023**, *16*, 3856. [[CrossRef](#)]
37. Zhen, L.; Lu, L.; Yao, Y.; Liu, J.; Yang, B. Flexible Inorganic Piezoelectric Functional Films and Their Applications. *J. Adv. Ceram.* **2023**, *12*, 433–462. [[CrossRef](#)]
38. Liu, Y.; Ding, L.; Dai, L.; Gao, X.; Wu, H.; Wang, S.; Zhuang, C.; Cai, L.; Liu, Z.; Liu, L.; et al. All-Ceramic Flexible Piezoelectric Energy Harvester. *Adv. Funct. Mater.* **2022**, *32*, 2209297. [[CrossRef](#)]
39. Xu, Q.; Tao, Y.; Wang, Z.; Zeng, H.; Yang, J.; Li, Y.; Zhao, S.; Tang, P.; Zhang, J.; Yan, M.; et al. Highly Flexible, High-Performance, and Stretchable Piezoelectric Sensor Based on a Hierarchical Droplet-Shaped Ceramics with Enhanced Damage Tolerance. *Adv. Mater.* **2024**, *36*, 2311624. [[CrossRef](#)]
40. Park, K.-I.; Son, J.H.; Hwang, G.-T.; Jeong, C.K.; Ryu, J.; Koo, M.; Choi, I.; Lee, S.H.; Byun, M.; Wang, Z.L.; et al. Highly-Efficient, Flexible Piezoelectric PZT Thin Film Nanogenerator on Plastic Substrates. *Adv. Mater.* **2014**, *26*, 2514–2520. [[CrossRef](#)]
41. Yan, J.; Han, Y.; Xia, S.; Wang, X.; Zhang, Y.; Yu, J.; Ding, B. Polymer Template Synthesis of Flexible BaTiO₃ Crystal Nanofibers. *Adv. Funct. Mater.* **2019**, *29*, 1907919. [[CrossRef](#)]
42. Yi, Z.; Zhang, W.; Yang, B. Flexible Piezo-Mems Fabrication Process Based on Thinned Piezoelectric Thick Film. In Proceedings of the 2021 IEEE 34th International Conference on Micro Electro Mechanical Systems (MEMS), Gainesville, FL, USA, 25–29 January 2021; pp. 670–673.
43. Zhou, X.; Parida, K.; Halevi, O.; Liu, Y.; Xiong, J.; Magdassi, S.; Lee, P.S. All 3D-Printed Stretchable Piezoelectric Nanogenerator with Non-Protruding Kirigami Structure. *Nano Energy* **2020**, *72*, 104676. [[CrossRef](#)]
44. Ji, B.; Xie, Z.; Hong, W.; Jiang, C.; Guo, Z.; Wang, L.; Wang, X.; Yang, B.; Liu, J. Stretchable Parylene-C Electrodes Enabled by Serpentine Structures on Arbitrary Elastomers by Silicone Rubber Adhesive. *J. Materiomics* **2020**, *6*, 330–338. [[CrossRef](#)]
45. Di Giorgio, C.; Blundo, E.; Pettinari, G.; Felici, M.; Bobba, F.; Polimeni, A. Mechanical, Elastic, and Adhesive Properties of Two-Dimensional Materials: From Straining Techniques to State-of-the-Art Local Probe Measurements. *Adv. Mater. Interfaces* **2022**, *9*, 2102220. [[CrossRef](#)]
46. Hinchet, R.; Khan, U.; Falconi, C.; Kim, S.-W. Piezoelectric Properties in Two-Dimensional Materials: Simulations and Experiments. *Mater. Today* **2018**, *21*, 611–630. [[CrossRef](#)]
47. Zhang, D.; Yang, Z.; Li, P.; Pang, M.; Xue, Q. Flexible Self-Powered High-Performance Ammonia Sensor Based on Au-Decorated MoSe₂ Nanoflowers Driven by Single Layer MoS₂-Flake Piezoelectric Nanogenerator. *Nano Energy* **2019**, *65*, 103974. [[CrossRef](#)]
48. Kou, J.; Liu, Y.; Zhu, Y.; Zhai, J. Progress in Piezotronics of Transition-Metal Dichalcogenides. *J. Phys. Appl. Phys.* **2018**, *51*, 493002. [[CrossRef](#)]
49. Habib, M.; Lantgios, I.; Hornbostel, K. A Review of Ceramic, Polymer and Composite Piezoelectric Materials. *J. Phys. Appl. Phys.* **2022**, *55*, 423002. [[CrossRef](#)]
50. Zhang, X.; Xia, W.; Liu, J.; Zhao, M.; Li, M.; Xing, J. PVDF-Based and Its Copolymer-Based Piezoelectric Composites: Preparation Methods and Applications. *J. Electron. Mater.* **2022**, *51*, 5528–5549. [[CrossRef](#)]
51. Jeong, C.K.; Baek, C.; Kingon, A.I.; Park, K.-I.; Kim, S.-H. Lead-Free Perovskite Nanowire-Employed Piezopolymer for Highly Efficient Flexible Nanocomposite Energy Harvester. *Small* **2018**, *14*, 1704022. [[CrossRef](#)]
52. Liu, X.-L.; Li, D.; Zhao, H.-X.; Dong, X.-W.; Long, L.-S.; Zheng, L.-S. Inorganic–Organic Hybrid Molecular Materials: From Multiferroic to Magnetoelectric. *Adv. Mater.* **2021**, *33*, 2004542. [[CrossRef](#)] [[PubMed](#)]
53. Bagheri, M.H.; Khan, A.A.; Shahzadi, S.; Rana, M.M.; Hasan, M.S.; Ban, D. Advancements and Challenges in Molecular/Hybrid Perovskites for Piezoelectric Nanogenerator Application: A Comprehensive Review. *Nano Energy* **2024**, *120*, 109101. [[CrossRef](#)]
54. Jella, V.; Ippili, S.; Yoon, S.-G. Halide (Cl/Br)-Incorporated Organic–Inorganic Metal Trihalide Perovskite Films: Study and Investigation of Dielectric Properties and Mechanical Energy Harvesting Performance. *ACS Appl. Electron. Mater.* **2020**, *2*, 2579–2590. [[CrossRef](#)]

55. Sayfidinov, K.; Cezan, S.D.; Baytekin, B.; Baytekin, H.T. Minimizing Friction, Wear, and Energy Losses by Eliminating Contact Charging. *Sci. Adv.* **2018**, *4*, eaau3808. [[CrossRef](#)] [[PubMed](#)]
56. Wang, Z.L.; Wang, A.C. On the Origin of Contact-Electrification. *Mater. Today* **2019**, *30*, 34–51. [[CrossRef](#)]
57. Hatta, F.F.; Mohammad Haniff, M.A.S.; Mohamed, M.A. A Review on Applications of Graphene in Triboelectric Nanogenerators. *Int. J. Energy Res.* **2022**, *46*, 544–576. [[CrossRef](#)]
58. Wang, J.; Li, X.; Zi, Y.; Wang, S.; Li, Z.; Zheng, L.; Yi, F.; Li, S.; Wang, Z.L. A Flexible Fiber-Based Supercapacitor–Triboelectric–Nanogenerator Power System for Wearable Electronics. *Adv. Mater.* **2015**, *27*, 4830–4836. [[CrossRef](#)]
59. Jiang, D.; Lian, M.; Xu, M.; Sun, Q.; Xu, B.B.; Thabet, H.K.; El-Bahy, S.M.; Ibrahim, M.M.; Huang, M.; Guo, Z. Advances in Triboelectric Nanogenerator Technology–Applications in Self-Powered Sensors, Internet of Things, Biomedicine, and Blue Energy. *Adv. Compos. Hybrid Mater.* **2023**, *6*, 57. [[CrossRef](#)]
60. Chen, H.; Xing, C.; Li, Y.; Wang, J.; Xu, Y. Triboelectric Nanogenerators for a Macro-Scale Blue Energy Harvesting and Self-Powered Marine Environmental Monitoring System. *Sustain. Energy Fuels* **2020**, *4*, 1063–1077. [[CrossRef](#)]
61. Wu, C.; Wang, A.C.; Ding, W.; Guo, H.; Wang, Z.L. Triboelectric Nanogenerator: A Foundation of the Energy for the New Era. *Adv. Energy Mater.* **2019**, *9*, 1802906. [[CrossRef](#)]
62. Li, X.; Xu, L.; Wang, Z.L. Networking Strategies of Triboelectric Nanogenerators for Harvesting Ocean Blue Energy. *Nanoenergy Adv.* **2024**, *4*, 70–96. [[CrossRef](#)]
63. Ravichandran, A.N.; Ramuz, M.; Blayac, S. Metal Island Structure as a Power Booster for High-Performance Triboelectric Nanogenerators. *Adv. Mater. Technol.* **2020**, *5*, 2000650. [[CrossRef](#)]
64. Park, J.; Cho, H.; Lee, Y.-S. Enhancing the Triboelectric Nanogenerator Output by Micro Plasma Generation in a Micro-Cracked Surface Structure. *Appl. Sci.* **2021**, *11*, 4262. [[CrossRef](#)]
65. Zhang, J.-H.; Li, Z.; Shen, B.; Liu, Z.; Chen, L.; Wang, H.; Li, H.; Zhang, Y.; Du, S.; Tang, Q.; et al. Electric Displacement Modulation under Internal Field for High-Performance Mechanical-to-Electrical Energy Generator. *Cell Rep. Phys. Sci.* **2024**, *5*, 102025. [[CrossRef](#)]
66. Kim, D.W.; Lee, J.H.; You, I.; Kim, J.K.; Jeong, U. Adding a Stretchable Deep-Trap Interlayer for High-Performance Stretchable Triboelectric Nanogenerators. *Nano Energy* **2018**, *50*, 192–200. [[CrossRef](#)]
67. Lin, L.; Wang, S.; Xie, Y.; Jing, Q.; Niu, S.; Hu, Y.; Wang, Z.L. Segmentally Structured Disk Triboelectric Nanogenerator for Harvesting Rotational Mechanical Energy. *Nano Lett.* **2013**, *13*, 2916–2923. [[CrossRef](#)]
68. Wang, F.; Wang, Z.; Zhou, Y.; Fu, C.; Chen, F.; Zhang, Y.; Lu, H.; Wu, Y.; Chen, L.; Zheng, H. Windmill-Inspired Hybridized Triboelectric Nanogenerators Integrated with Power Management Circuit for Harvesting Wind and Acoustic Energy. *Nano Energy* **2020**, *78*, 105244. [[CrossRef](#)]
69. Meng, B.; Tang, W.; Zhang, X.; Han, M.; Liu, W.; Zhang, H. Self-Powered Flexible Printed Circuit Board with Integrated Triboelectric Generator. *Nano Energy* **2013**, *2*, 1101–1106. [[CrossRef](#)]
70. Prasad, G.; Graham, S.A.; Yu, J.S.; Kim, H.; Lee, D.-W. Investigated a PLL Surface-Modified Nylon 11 Electrospun as a Highly Tribo-Positive Frictional Layer to Enhance Output Performance of Triboelectric Nanogenerators and Self-Powered Wearable Sensors. *Nano Energy* **2023**, *108*, 108178. [[CrossRef](#)]
71. Wang, F.; Ke, S.; Li, J.; Zhang, J.-H.; Cheng, Y.; Huang, J.; Shi, Y.; Pan, L. Adaptively Responsive Self-Powered Bionic Auditory Device for Sleep Health Monitoring. *IEEE Electron Device Lett.* **2023**, *44*, 1348–1351. [[CrossRef](#)]
72. Zhang, J.-H.; Li, Z.; Xu, J.; Li, J.; Yan, K.; Cheng, W.; Xin, M.; Zhu, T.; Du, J.; Chen, S.; et al. Versatile Self-Assembled Electrospun Micropyramid Arrays for High-Performance on-Skin Devices with Minimal Sensory Interference. *Nat. Commun.* **2022**, *13*, 5839. [[CrossRef](#)]
73. Yu, Y.; Wang, X. Chemical Modification of Polymer Surfaces for Advanced Triboelectric Nanogenerator Development. *Extreme Mech. Lett.* **2016**, *9*, 514–530. [[CrossRef](#)]
74. Jing, Q.; Kar-Narayan, S. Nanostructured Polymer-Based Piezoelectric and Triboelectric Materials and Devices for Energy Harvesting Applications. *J. Phys. Appl. Phys.* **2018**, *51*, 303001. [[CrossRef](#)]
75. Lin, Q.; Wang, L. Layered Double Hydroxides as Electrode Materials for Flexible Energy Storage Devices. *J. Semicond.* **2023**, *44*, 041601–041616. [[CrossRef](#)]
76. Fan, J.; Yuan, M.; Wang, L.; Xia, Q.; Zheng, H.; Zhou, A. MXene Supported by Cotton Fabric as Electrode Layer of Triboelectric Nanogenerators for Flexible Sensors. *Nano Energy* **2023**, *105*, 107973. [[CrossRef](#)]
77. Li, C.; Wang, P.; Zhang, D. Self-Healable, Stretchable Triboelectric Nanogenerators Based on Flexible Polyimide for Energy Harvesting and Self-Powered Sensors. *Nano Energy* **2023**, *109*, 108285. [[CrossRef](#)]
78. Han, S.A.; Lee, J.; Lin, J.; Kim, S.-W.; Kim, J.H. Piezo/Triboelectric Nanogenerators Based on 2-Dimensional Layered Structure Materials. *Nano Energy* **2019**, *57*, 680–691. [[CrossRef](#)]
79. Seol, M.; Kim, S.; Cho, Y.; Byun, K.-E.; Kim, H.; Kim, J.; Kim, S.K.; Kim, S.-W.; Shin, H.-J.; Park, S. Triboelectric Series of 2D Layered Materials. *Adv. Mater.* **2018**, *30*, 1801210. [[CrossRef](#)]
80. Zhou, Y.; Zhang, J.-H.; Li, S.; Qiu, H.; Shi, Y.; Pan, L. Triboelectric Nanogenerators Based on 2D Materials: From Materials and Devices to Applications. *Micromachines* **2023**, *14*, 1043. [[CrossRef](#)]
81. Xia, X.; Chen, J.; Liu, G.; Javed, M.S.; Wang, X.; Hu, C. Aligning Graphene Sheets in PDMS for Improving Output Performance of Triboelectric Nanogenerator. *Carbon* **2017**, *111*, 569–576. [[CrossRef](#)]

82. Wu, C.; Kim, T.W.; Choi, H.Y. Reduced Graphene-Oxide Acting as Electron-Trapping Sites in the Friction Layer for Giant Triboelectric Enhancement. *Nano Energy* **2017**, *32*, 542–550. [[CrossRef](#)]
83. Yang, P.; Wang, P.; Diao, D. Graphene Nanosheets Enhanced Triboelectric Output Performances of PTFE Films. *ACS Appl. Electron. Mater.* **2022**, *4*, 2839–2850. [[CrossRef](#)]
84. Park, S.; Park, J.; Kim, Y.; Bae, S.; Kim, T.-W.; Park, K.-I.; Hong, B.H.; Jeong, C.K.; Lee, S.-K. Laser-Directed Synthesis of Strain-Induced Crumpled MoS₂ Structure for Enhanced Triboelectrification toward Haptic Sensors. *Nano Energy* **2020**, *78*, 105266. [[CrossRef](#)]
85. Cai, Y.-W.; Zhang, X.-N.; Wang, G.-G.; Li, G.-Z.; Zhao, D.-Q.; Sun, N.; Li, F.; Zhang, H.-Y.; Han, J.-C.; Yang, Y. A Flexible Ultra-Sensitive Triboelectric Tactile Sensor of Wrinkled PDMS/MXene Composite Films for E-Skin. *Nano Energy* **2021**, *81*, 105663. [[CrossRef](#)]
86. Xu, R.; Luo, F.; Zhu, Z.; Li, M.; Chen, B. Flexible Wide-Range Triboelectric Sensor for Physiological Signal Monitoring and Human Motion Recognition. *ACS Appl. Electron. Mater.* **2022**, *4*, 4051–4060. [[CrossRef](#)]
87. Panda, S.; Hajra, S.; Song, H.; Jo, J.; Kim, N.; Hwang, S.; Choi, Y.; Kim, H.G.; Kim, H.J.; Mishra, Y.K. Pyroelectric Based Energy Harvesting Devices: Hybrid Structures and Applications. *Sustain. Energy Fuels* **2023**, *7*, 5319–5335. [[CrossRef](#)]
88. Korkmaz, S.; Kariper, İ.A. Pyroelectric Nanogenerators (PyNGs) in Converting Thermal Energy into Electrical Energy: Fundamentals and Current Status. *Nano Energy* **2021**, *84*, 105888. [[CrossRef](#)]
89. Ryu, H.; Kim, S.-W. Emerging Pyroelectric Nanogenerators to Convert Thermal Energy into Electrical Energy. *Small* **2021**, *17*, 1903469. [[CrossRef](#)]
90. Bowen, C.R.; Taylor, J.; LeBoulbar, E.; Zabek, D.; Chauhan, A.; Vaish, R. Pyroelectric Materials and Devices for Energy Harvesting Applications. *Energy Environ. Sci.* **2014**, *7*, 3836–3856. [[CrossRef](#)]
91. Zhang, D.; Wu, H.; Bowen, C.R.; Yang, Y. Recent Advances in Pyroelectric Materials and Applications. *Small* **2021**, *17*, 2103960. [[CrossRef](#)]
92. He, H.; Lu, X.; Hanc, E.; Chen, C.; Zhang, H.; Lu, L. Advances in Lead-Free Pyroelectric Materials: A Comprehensive Review. *J. Mater. Chem. C* **2020**, *8*, 1494–1516. [[CrossRef](#)]
93. Sultana, A.; Ghosh, S.K.; Alam, M.M.; Sadhukhan, P.; Roy, K.; Xie, M.; Bowen, C.R.; Sarkar, S.; Das, S.; Middya, T.R.; et al. Methylammonium Lead Iodide Incorporated Poly(Vinylidene Fluoride) Nanofibers for Flexible Piezoelectric–Pyroelectric Nanogenerator. *ACS Appl. Mater. Interfaces* **2019**, *11*, 27279–27287. [[CrossRef](#)] [[PubMed](#)]
94. Wu, Y.; Du, X.; Gao, R.; Li, J.; Li, W.; Yu, H.; Jiang, Z.; Wang, Z.; Tai, H. Self-Polarization of PVDF Film Triggered by Hydrophilic Treatment for Pyroelectric Sensor with Ultra-Low Piezoelectric Noise. *Nanoscale Res. Lett.* **2019**, *14*, 72. [[CrossRef](#)] [[PubMed](#)]
95. Lee, J.; Kim, H.J.; Ko, Y.J.; Baek, J.Y.; Shin, G.; Jeon, J.G.; Lee, J.H.; Kim, J.H.; Jung, J.H.; Kang, T.J. Enhanced Pyroelectric Conversion of Thermal Radiation Energy: Energy Harvesting and Non-Contact Proximity Sensor. *Nano Energy* **2022**, *97*, 107178. [[CrossRef](#)]
96. Guan, H.; Li, W.; Yang, R.; Su, Y.; Li, H. Microstructured PVDF Film with Improved Performance as Flexible Infrared Sensor. *Sensors* **2022**, *22*, 2730. [[CrossRef](#)] [[PubMed](#)]
97. Yang, R.; Zhang, W.; Tiwari, N.; Yan, H.; Li, T.; Cheng, H. Multimodal Sensors with Decoupled Sensing Mechanisms. *Adv. Sci.* **2022**, *9*, 2202470. [[CrossRef](#)] [[PubMed](#)]
98. Shin, Y.-E.; Sohn, S.-D.; Han, H.; Park, Y.; Shin, H.-J.; Ko, H. Self-Powered Triboelectric/Pyroelectric Multimodal Sensors with Enhanced Performances and Decoupled Multiple Stimuli. *Nano Energy* **2020**, *72*, 104671. [[CrossRef](#)]
99. Roy, K.; Ghosh, S.K.; Sultana, A.; Garain, S.; Xie, M.; Bowen, C.R.; Henkel, K.; Schmeißer, D.; Mandal, D. A Self-Powered Wearable Pressure Sensor and Pyroelectric Breathing Sensor Based on GO Interfaced PVDF Nanofibers. *ACS Appl. Nano Mater.* **2019**, *2*, 2013–2025. [[CrossRef](#)]
100. Chen, C.; Zhao, S.; Pan, C.; Zi, Y.; Wang, F.; Yang, C.; Wang, Z.L. A Method for Quantitatively Separating the Piezoelectric Component from the As-Received “Piezoelectric” Signal. *Nat. Commun.* **2022**, *13*, 1391. [[CrossRef](#)]

Disclaimer/Publisher’s Note: The statements, opinions and data contained in all publications are solely those of the individual author(s) and contributor(s) and not of MDPI and/or the editor(s). MDPI and/or the editor(s) disclaim responsibility for any injury to people or property resulting from any ideas, methods, instructions or products referred to in the content.